Overall Project title: [Theoretical and experimental research in the origin of turbulence]

ENGINEERING EXPERIMENT STATION
of the Georgia Institute of Technology
Atlanta, Georgia

PROJECT NO. 219

A REPORT ON THE DESIGN, CONSTRUCTION, OPERATION AND PRELIMINARY CALIBRATIONS ON THE LOW TURBULENCE WIND TUNNEL AT THE GEORGIA INSTITUTE OF TECHNOLOGY.

By

ARNOLD L. DUCOFFE
Daniel Guggenheim School of Aeronautics

- 0 - 0 - 0 - 0 - 0 - 0 - 0 -

NAVY DEPARTMENT, OFFICE OF NAVAL RESEARCH

CONTRACT NO. Nonr-991(01)

- 0 - 0 - 0 - 0 - 0 - 0 - 0 -

MAY - 1956

TABLE OF CONTENTS

	Page
SUMMARY	1
INTRODUCTION	1
DESCRIPTION OF LOW TURBULENCE WIND TUNNEL	1
Fan Unit	2
Transition Section	2
Wide Angle Diffuser	3
Settling Chamber	3
Contraction Cone	3
Working Section	3
DESCRIPTION OF INSTRUMENTATION	4
CALIBRATION TESTS	6
Future Work	6
PERSONNEL	7
FIGURES 1 through 10	8-14

A REPORT ON THE DESIGN, CONSTRUCTION, OPERATION AND PRELIMINARY CALIBRATIONS ON THE LOW TURBULENCE WIND TUNNEL AT THE GEORGIA INSTITUTE OF TECHNOLOGY

By Arnold L. Ducoffe

Georgia Institute of Technology

SUMMARY

This report presents information on the design, construction, operation and preliminary calibration data on the Low Turbulence Wind Tunnel at the Georgia Institute of Technology.

The initial calibration results seem to indicate that the flow properties in the tunnel will satisfy basic requirements. No statements concerning the turbulence level can be made at this time.

INTRODUCTION

The construction of the Low Turbulence Wind Tunnel, using Georgia Tech funds, was initiated in July 1953. The construction of the tunnel shell, the installation of the fan, and the installation of the turbulence damping screens were completed by September 1954. Because of a lack of funds progress during the period September 1954 - September 1955 was curtailed. However, during this period the probe carrier mechanism was installed in the tunnel and the power controls, as well as the remote controls for the probe carrier, were designed and constructed. On or about October 15, 1955 the design of the pressure calibration and hot wire anemometer probes were undertaken and built. In addition, probe position indicators were installed.

The calibration of the tunnel began during the middle of April and has proceeded from that time.

DESCRIPTION OF LOW TURBULENCE WIND TUNNEL

The tunnel is of the Eiffel type (i.e. the room in which the tunnel is housed serves as the return leg for the flow). The design incorporates the following segments as shown reading from left to right in Figure 1:

a. Fan unit
b. Transition section
c. Wide angle diffuser
d. Settling chamber
e. Contraction cone
f. Working section

Fan Unit

The fan is of the axial flow type having a diameter of 54 inches and capable of delivering 55,000 cubic feet of air against three inches of water pressure drop. The V-belts driving the fan are located upstream of the plane of rotation at a point where they pass through the entrance cone. The fan is powered by a 40 horsepower D.C. motor which is driven by a 50 horsepower A.C. induction motor driving a D.C. generator. This power system is essentially that of a Ward Leonard system with the exception that the A.C. motor in such a system is a synchroneous rather than induction type. The induction type motor was used because it was available from equipment which the school had acquired from government surplus stocks. The fan nacelle is approximately 27 inches in diameter. This nacelle terminates in a vertical plane at the fan exit. In order to eliminate the wake from the bluff end of the nacelle a fairing, which extends to the entrance of the wide angle diffuser, was added. The fairing is essentially an ogive with a blunt apex and was designed so that the diffusion angle in the transition section was maintained at less than 7 degrees for an equivalent conical diffuser. The front of the entrance cone is covered with 1/2 inch hardware cloth in order that it could be covered with cheese cloth to protect the damping screens from collecting dust.

Transition Section

The transition section is incorporated in order to accommodate a geometry change from a round cross-section, 54 inches in diameter, to a square of the same area (48" x 48" approx.). The transition section is constructed of aluminum sheet with formed angles for attachment.

Wide Angle Diffuser

In order to provide for a large expansion in a short distance without separation, a wide angle diffuser is used. The wide angle diffuser has an entrance area of 15.92 square feet and an exit area of 121 square feet. The included angle between side walls is 77 degrees and the radius at the entrance is approximately 33 inches. Six Monel wire cloth screens (20 x 20 mesh with 0.009" diameter wire) are provided to expand the flow. The positioning of these screens for the most efficient expansion (without separation) was determined prior to the tunnel construction by a master's degree candidate. The work resulted in his master's thesis. The screens are installed so that each may be easily removed for cleaning purposes and replacement if damaged.

Settling Chambers

The settling chamber measures 11 feet x 11 feet and is equipped with 6 - 24 mesh square weave phosphor bronze screens with 0.0075" diameter wire. Provision is made for easy removal of these screens for the same reasons as discussed under wide angle diffuser screens. In addition, screen frames are installed in the settling chamber to accommodate two additional screens if deemed necessary after calibration. A honeycomb made from hex aluminum extrusions (8 inches long x 2 inches across the flats) is provided at the entrance of the settling chamber.

Contraction Cone

The contraction cone is designed with an 11:1 contraction ratio. The shape of the cone was derived from a fourth degree curve with the point of inflection located approximately one foot from the entrance and the first and second derivatives (dy/dx, d^2y/dx^2) being zero at the exit end.

Working Section

The working section is 3 1/2 feet x 3 1/2 feet x 20 feet in length. One vertical wall is constructed of plexiglass and the other vertical wall is formed by a single sheet of 24 ST aluminum. This latter wall is moveable. At the entrance to the working section the moveable wall is

attached to a vertical solid steel shaft. This shaft has a camlike cross-section in order to accommodate the movable wall. Thus, as the wall is moved, the shaft rotates always presenting a smooth surface for the air flow. Five jacks are attached to the movable wall to provide means for controlling its shape and position. The maximum limit for each jack is $\pm$ 21 inches. The ceiling and floor of the working section are constructed from aluminum covered plywood in order to facilitate the movement of the probe carrier which will be described later.

The tunnel is completely shock-mounted by rubber pads provided for all footings. Vibrations from the fan assembly are eliminated by the use of two inches of sponge rubber between the fan housing and the transition section. Windows are provided in the transition section, wide angle diffuser, settling chamber, and in the working section. Interior lights are provided in the settling chamber. The entrance and exit of the tunnel are located 48 inches and 128 inches respectively from the walls of the building. The tunnel runs from west to east--the entrance being at the west end. Figures 2 and 3 (looking north) give a photographic description of the tunnel.

DESCRIPTION OF INSTRUMENTATION

The probe carrier is designed so that it may be moved east-west and north-south by remote control. The vertical position is changed manually. Photographically, Figure 4 shows the probe and probe carrier mounted in the tunnel. The design incorporates two 20 foot aluminum channels; one on the floor and the other on the ceiling of the working section. The legs of each channel face one another. The channels are fastened at each end of the working section to a N - S positioning mechanism. Provision is made for the probe carrier to be moved $\pm$ 18 inches from the tunnel centerline. The channels on the floor and ceiling are moved by lead screws which are driven by a single chain drive. Thus parallel motion is assured. The E - W motion is accomplished by chain drives which are housed in the top and bottom channels. In order to guide the probe carrier in its E - W movement, two pieces of formica are milled to

travel along the legs of each channel thus preventing any twisting of the carrier. The probe carrier is built with a lead screw for vertical positioning. A nut on the lead screw allows for holding the probe. Reversible motors are used so that the positioning of the probe carrier can be easily accomplished. In addition, a hand crank is provided for N - S travel so that the probe can be positioned, near a flat plate, with a large degree of accuracy. The probe carrier is also equipped with an Ames dial gauge indicator which has a capability of measuring to 0.0001 inch with an inch travel. The total head and hot-wire boundary layer probes are equipped with needle-like pointers. When these pointers contact the flat metal wall of the tunnel, a light will flash and then the distance from the wall will be measured with the dial indicator. Limit switches are provided in the E - W and N - S travel directions in order that the mechanism is protected.

Typical features of the probes to be used are shown in Figure 5. The distance sensing needles on both the total head and hot-wire probes are shown in the figure.

The tunnel control console is shown in Figure 6. The panel consists of motor controls on the left side and probe position controls on the right side. On the left of the control table the manometry which will be used for pressure measurements is shown. These manometers, designed at Georgia Tech, are capable of detecting 0.001 inch of alcohol without difficulty.

The hot-wire anemometer equipment was purchased from Thiele Instruments, Inc. and is shown in Figure 7.

Piezometer rings at the entrance and at the exit of the contraction cone are provided for speed calibration.

In order to provide take-up on the pressure tubing as the probe moves toward the tunnel exit a series of pulleys have been installed on the ceiling of the room. A counterweight is also provided near the east wall of the building in order to maintain constant tension on the tubing.

CALIBRATION TESTS

The calibration of the tunnel began about the middle of April. As is normal on this type of equipment, certain difficulties had to be worked out of the system. It was decided that the initial phases of the calibration program consist of a speed survey, an angularity survey, a dynamic pressure survey, and a longitudinal pressure survey.

The speed survey (Figure 8) indicates that the tunnel is capable of a maximum speed of approximately 70 feet/sec. Since the purpose of the tunnel is not to provide high velocities, this value is believed to be satisfactory.

Because the initial tests (after calibration) are to be conducted on a flat plate, it was desired to determine whether the longitudinal static pressure gradient in the tunnel could be eliminated by proper positioning of the movable wall. The results of a preliminary investigation are shown in Figure 9, wherein it is noted that with slight adjustments a value of $dp/dx = 0$ is feasible.

A dynamic pressure survey was undertaken; the results of which are shown in Figure 10. However, during these runs it was noted that a surge in the dynamic pressure was present. At first this was attributed to the proximity of the walls of the building to the tunnel exit. Damping screens were installed at the exit (between the tunnel exit and the walls of the building) and a reduction in surge resulted. However, further investigation indicates that flapping of the pressure leads is sufficient to cause the surge. At present work is being carried on to enclose these leads. Additional tension on the tubing which must remain exposed within the tunnel will probably eliminate the remainder of the surge.

Future Work

It is proposed that the summer of 1956 be used to obtain complete pressure, angularity, and velocity surveys at low, moderate, and high speeds. In the fall the turbulence level will be determined and a flat plate inserted in the tunnel. A turbulent boundary layer will be generated by roughening of the plate leading edge. Velocity profiles and turbulence measurements will then be made with a zero longitudinal pressure gradient. Similar measurements will be made with positive and negative longitudinal pressure gradients.

PERSONNEL

The personnel working with the tunnel at present consist of the project director, Dr. A. L. Ducoffe, who is devoting 1/4 time, a graduate student devoting 1/2 time, and three undergraduate students devoting 3/4 time, 1/2 time and 1/2 time respectively. It is proposed that the work continue with a minimum of two students at all times.

The work on the tunnel has resulted in a master's thesis on the wide angle diffuser and, it is believed, two master's theses should result from the work to be carried on in the coming fiscal year.

Prepared by

APPROVED:

A. L. Ducoffe, Project Director

Thomas W. Jackson, Chief
Mechanical Sciences Division

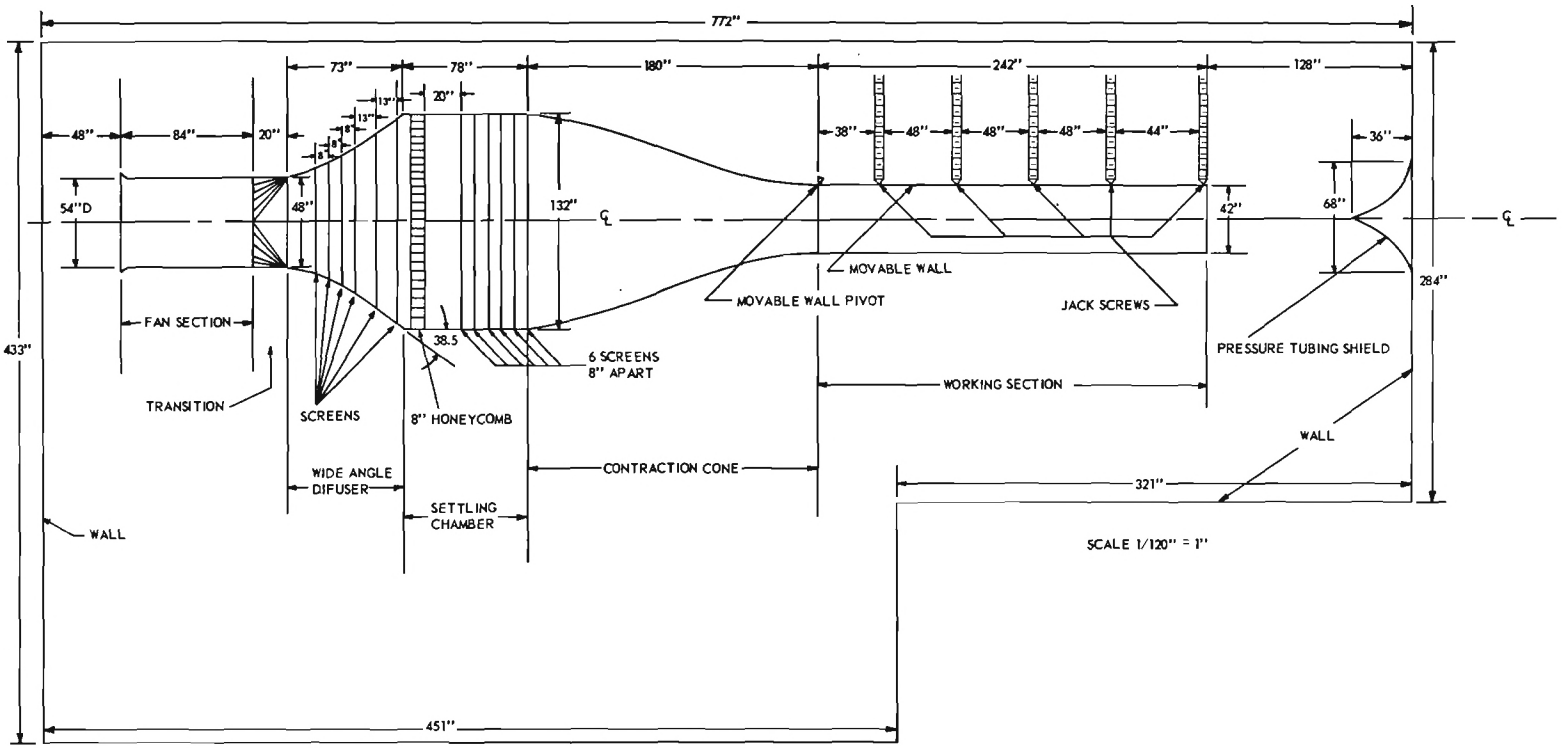

Figure 1. Schematic of Low Turbulence Wind Tunnel at Ga. Inst. of Tech.

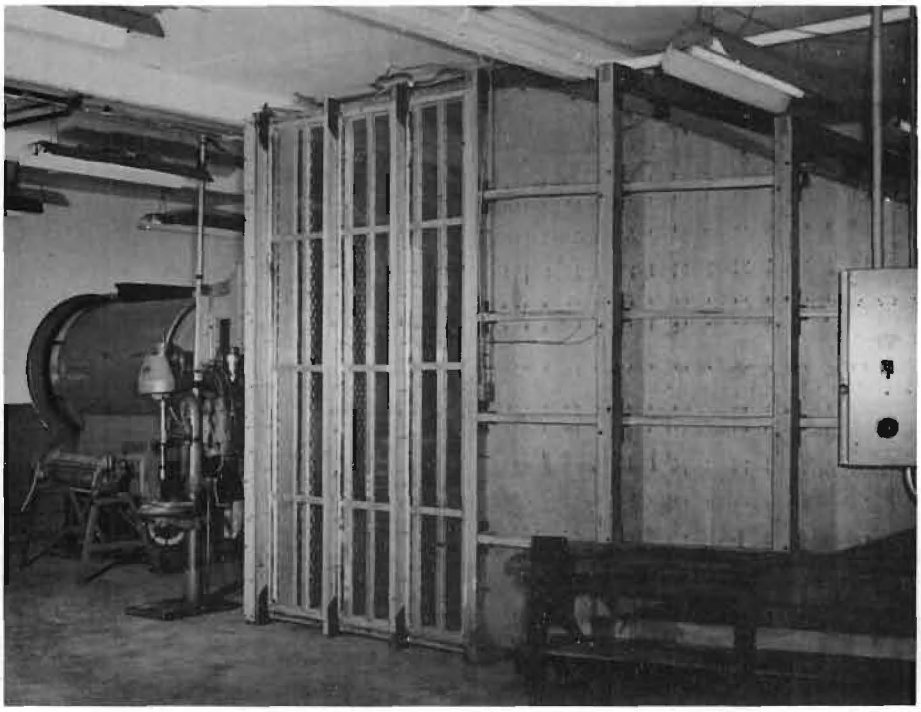

Figure 2. West End of Tunnel.

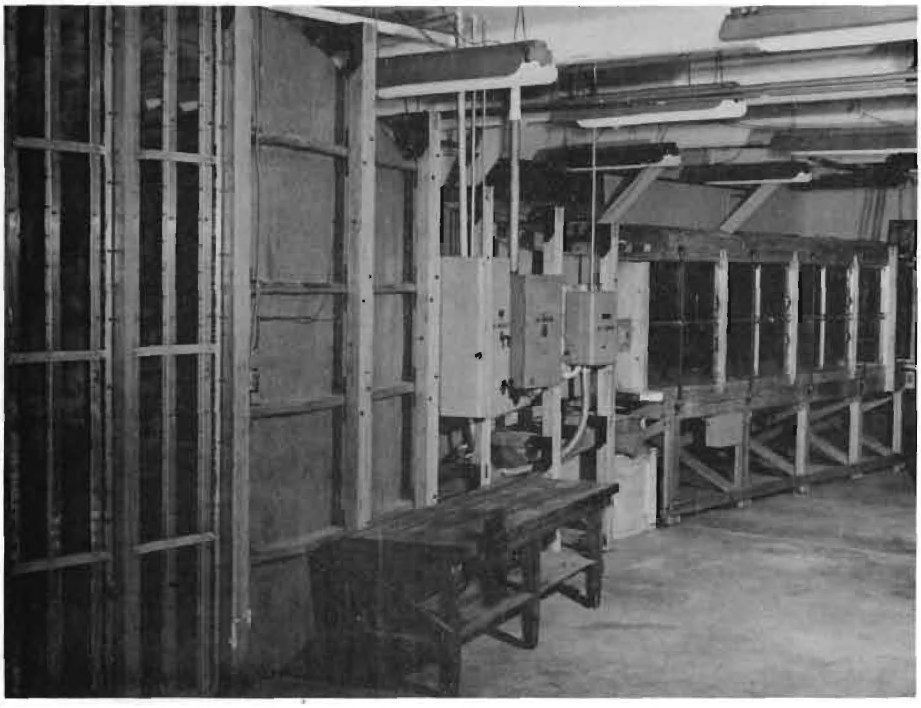

Figure 3. East End of Tunnel.

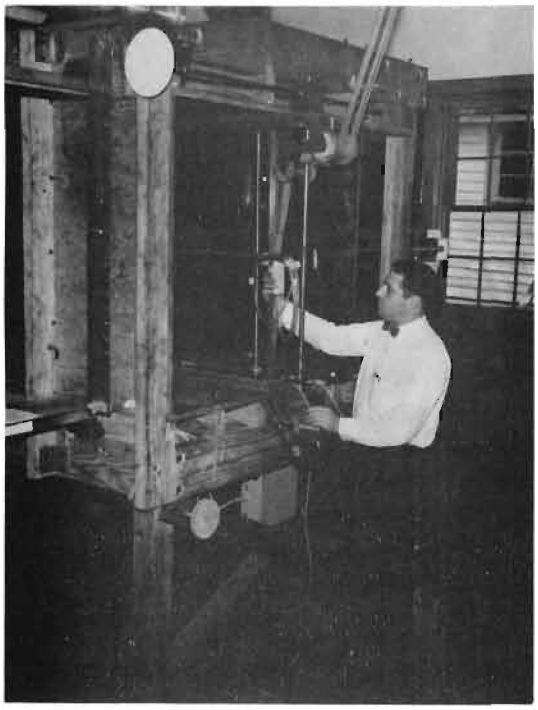

Figure 4. Probe Carrier at Tunnel Exit.

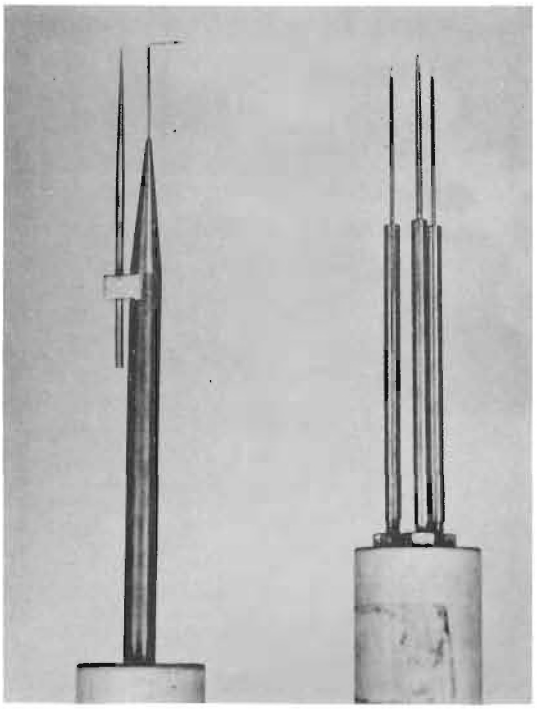

Figure 5. Total Head and Hot Wire Probes.

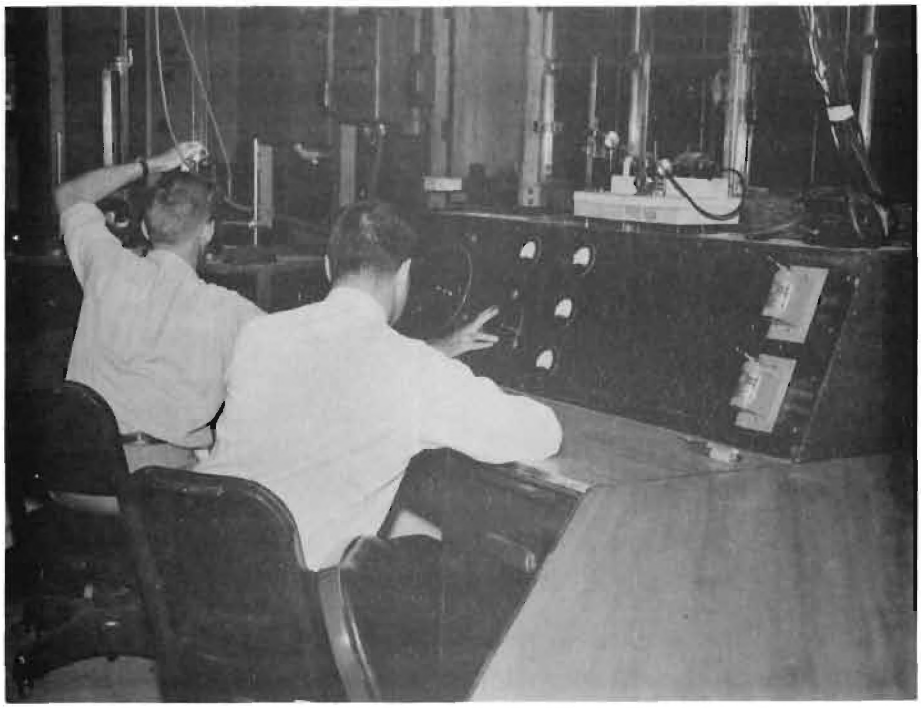

Figure 6. Tunnel Control Console.

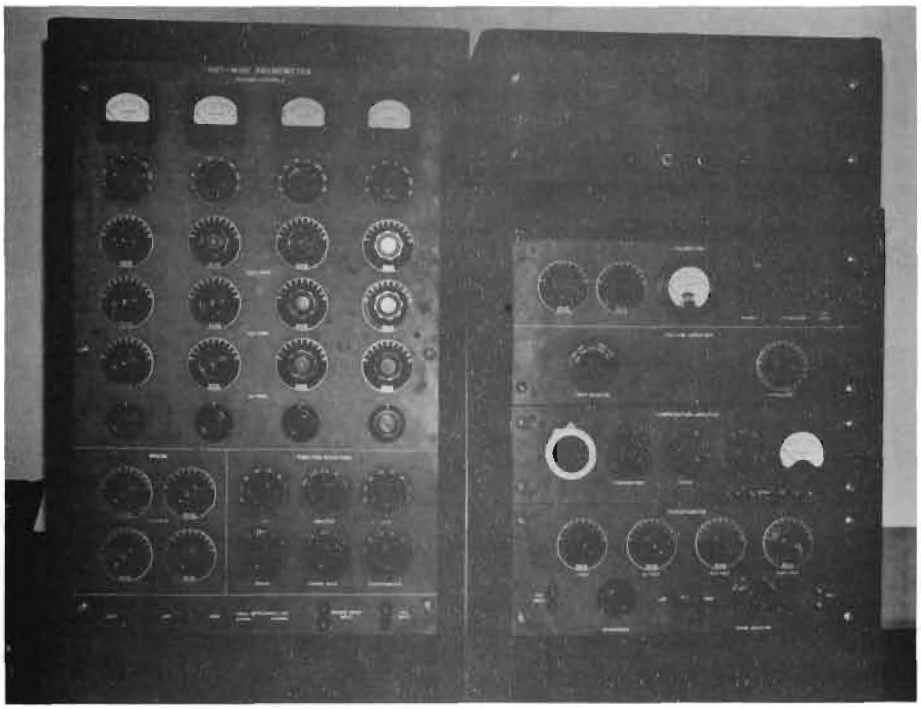

Figure 7. Hot Wire Equipment.

SPEED CALIBRATION PRELIMINARY

Fig. 8

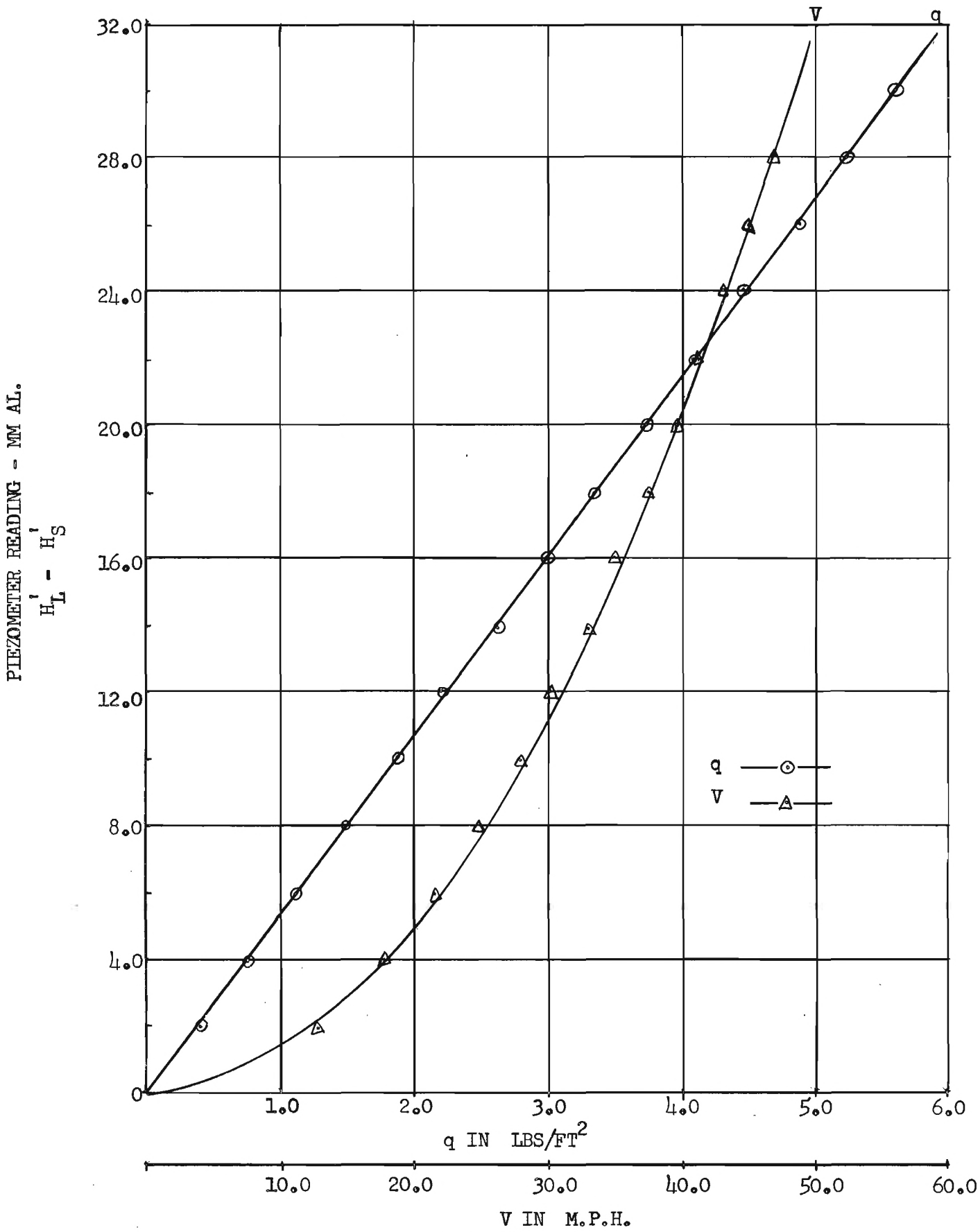

LONGITUDINAL STATIC PRESSURE

GRADIENT ALONG TUNNEL AXIS PRELIMINARY

PIEZOMETER = 10 mm AL

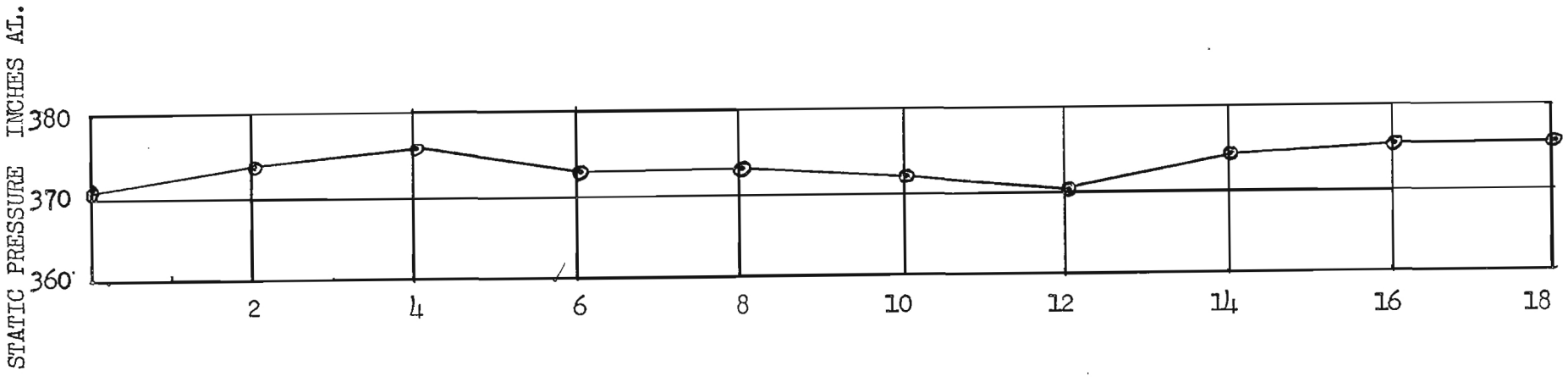

DISTANCE ALONG TUNNEL CENTERLINE - FT.

Range .006

Fig. 9

HORIZONTAL q SURVEY ALONG THE VERTICAL

CENTERLINE PROBE MOUNTED 6" DOWNSTREAM OF WORKING

SECTION ENTRANCE PRELIMINARY

PIEZOMETER - 20 mm AL

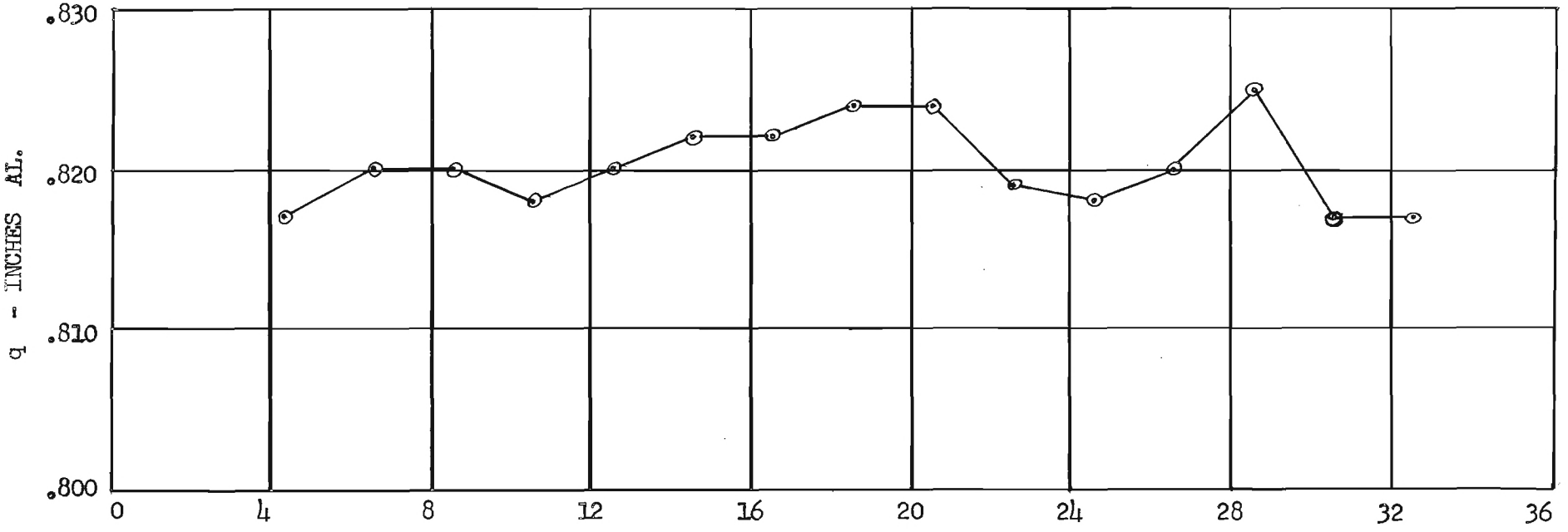

DISTANCE FROM CENTERLINE OF PROBE

TO STATIONARY WALL - INCHES

NOTE: All Readings Approximate Due to Surge

Fig. 10

Engineering Experiment Station

of the Georgia Institute of Technology

Atlanta, Georgia

Project No. 219

I A Report On the Final Calibration of the Low Turbulence Wind Tunnel Including Dynamic Pressure and Angularity Surveys and Free Tunnel Turbulence Measurements

II Turbulence Studies Behind Square Mesh Grids

III Boundary-Layer Velocity Profiles and Turbulence Studies on a Flat Plate in the Presence of a Zero Longitudinal Static Pressure Gradient

By

Arnold L. Ducoffe

Daniel Guggenheim School of Aeronautics

- o - o - o - o - o - o - o - o -

Navy Department, Office of Naval Research

Contract No. NOnr - 991(01)

- o - o - o - o - o - o -

July 1957

ACKNOWLEDGMENTS

The author wishes to express his appreciation to the following personnel for their invaluable help during the course of this project. Messrs. E. Flynt and B. Warren for their work with the hot-wire equipment, Mr. A. Ortell (graduate student) for his assistance in running the experiments and reducing the data, Mr. J. Van Tassel (undergraduate student) for his help in running the tunnel and taking data, and Mr. W. M. Rees for his efforts during the design and construction of the wind tunnel.

TABLE OF CONTENTS

	Page
ACKNOWLEDGMENTS	i
SUMMARY	1
NOTATION	3
INTRODUCTION	5
EXPERIMENTAL TESTS AND PROCEDURE	8
RESULTS	14
CONCLUSIONS	21
REFERENCES	23
FIGURES	24

SUMMARY

Data on the final calibration of the low turbulence wind tunnel are presented herein. These data include the variation in longitudinal static pressure gradient obtained with the moveable tunnel wall, dynamic pressure and angularity surveys, and free tunnel turbulence intensity. Measurements of the three components of turbulence behind one and two inch square mesh grids were made to evaluate the performance of the tunnel and hot-wire equipment. In addition, a flat plate with a roughened leading edge was installed and velocity profiles (zero longitudinal static pressure gradient) were measured at selected longitudinal stations by means of total head and hot-wire probes. Measurement of the intensity of the longitudinal component of turbulence through the boundary-layer at several longitudinal positions is also presented. All tests reported herein were run at a tunnel speed of 21 ft/sec.

The results indicate that the adjustment of the moveable wall is sufficiently flexible to give arbitrary longitudinal static pressure gradients accurate to within $\pm$ 0.002 inch of alcohol/foot of length. The dynamic pressure and angularity surveys are well within tolerable limits ($\pm$ 1/4 % q and $\pm$ 0.25 degrees) over a central core defined by Y = $\pm$ 15 and Z = $\pm$ 15 inches except at the extreme aft end of the tunnel where the open working section increases the range of deviation. The free tunnel turbulence increases from approximately 0.00016 for each of the three components at the entrance to the working section to a maximum of approximately 0.00062 for the w' component at the downstream end.

The turbulence measurements behind grids show good correlation with the results measured in other facilities.

The boundary-layer profiles on the flat plate show good agreement with the 1/7 power law. The intensity of the longitudinal component of turbulence in the boundary layer is seen to be strongly influenced by the presence of the artificial roughness in the vicinity of the roughness element. However, downstream of the roughness element the artificial turbulence decays rapidly and the distribution of the longitudinal component of turbulence in the boundary-layer is approximately defined by a single curve independent of axial position along the plate.

NOTATION

h_p	static pressure, inches of alcohol
Δh_p	static pressure at entrance to working section - static pressure at any spatial station, inches of alcohol
h_{p_z}	piezometer pressure, inches of alcohol
h_q	dynamic pressure, inches of alcohol
u, v, w	X, Y, and Z components of instantaneous turbulent velocity fluctuations
$\overline{u^2}, \overline{v^2}, \overline{w^2}$	mean-square values of u, v, and w
u', v', w'	root-mean-square values of u, v, and w
M	mesh size of grid, inches
R_{e_M}	Reynolds number, $\frac{\rho}{\mu} U_1 M$, based on mesh size
R_{e_X}	Reynolds number, $\frac{\rho}{\mu} U_1 X$, based on length, X
U	mean velocity in boundary-layer, ft/sec.
U_1	mean velocity in freestream, just outside boundary-layer
V_i	indicated airspeed, $U_1 \sigma^{1/2}$, in main stream
X	longitudinal spatial position, positive when moving upstream from working section entrance
Y	lateral spatial position, positive to the right looking upstream on $\mathbb{C}$

Z	vertical spatial position, positive upward looking upstream on $\mathcal{L}$
α	angle of flow in X-Z plane, positive upward when looking upstream
$\Delta\ \alpha$	difference in flow angle between centerline value and any lateral station in a given horizontal plane
δ	boundary-layer thickness
δ^*	boundary-layer displacement thickness, $\left(\int_0^\infty \left(1 - \frac{U}{U_1}\right) dy \right)$
θ	boundary-layer momentum thickness, $\left(\int_0^\infty \frac{U}{U_1} \left(1 - \frac{U}{U_1}\right) dy \right)$
μ	viscosity of air
ρ	mass density of air
ρ_o	mass density of air at sea level, 0.002378 slugs/ft^3
σ	ρ/ρ_o
ψ	angle of flow in X-Y plane, positive from left to right when looking upstream
$\Delta\ \psi$	difference in flow angle between centerline value and any lateral station in a given horizontal plane

INTRODUCTION

As outlined in reference 1 the construction of the low turbulence wind tunnel was completed in April 1956. The preliminary dynamic pressure and angularity surveys in the working section were conducted during the spring of 1956, and are summarized in reference 1. During the summer of 1956 more extensive dynamic pressure and angularity surveys were run. However, analysis of these surveys indicated undesirable dynamic pressure and angularity distributions, and also the tunnel exhibited a low frequency surge. A program to determine the cause of these undesirable features was initiated. After two months of detailed pitot-tube probing and tuft studies at the tunnel entrance, in the wide angle diffuser, and at the tunnel exit, two modifications to the tunnel were made. The first modification involved the bell-mouth or entrance area of the tunnel. During the investigation of this area two undesirable characteristics were found, namely, the hardware-cloth which was stretched across the bell-mouth to support the cheese-cloth was vibrating, and the air entering the bell-mouth area possessed a great deal of rotation. In order to eliminate the use of hardware-cloth but still use cheese-cloth as a filter for dust and debris and also to eliminate the rotation of entering tunnel air, a set of 16 anti-twist vanes was installed. These vanes were made of 1/4 inch plywood and measured 48 inches in length by 12 inches wide. The vanes were mounted with the 48 inch dimension spanning the distance between the bell-mouth and the wall of the room. The vanes were mounted radially about the tunnel centerline and were attached to the bell-mouth and wall by means of pins in order

that they might be pivoted to provide for angular changes. Locking devices in the form of adjustable angle iron clips were also provided to maintain the optimum angle setting for each vane. The outer perimeter provided a means for locating the cheese-cloth and also reduced the pressure drop through the cheese-cloth since this area exists in a very low velocity region compared to the bell-mouth plane. The second modification resulted from tuft studies between the exit of the fan section and the entrance to the wide angle diffuser. As reported in reference 1 the fan unit was modified by extending the fan nacelle back into the wide-angle diffuser by means of an ogive with a blunt apex. Tuft studies near the apex (which was located immediately in front of the first screen in the wide-angle diffuser) indicated that the aft portion of the nacelle was stalled. In order to eliminate the nacelle stall an 18 x 14 mesh screen was stretched across the tunnel approximately eight inches upstream of the nacelle apex. The 18 x 14 mesh screen was installed with a hole cut in the center so that the perimeter of the hole conformed to the nacelle contour. Preliminary velocity surveys in the working section indicated that the corrective measures described above had essentially eliminated the surge at low speeds, reduced the surge magnitude to within tolerable limits at high speed, and also smoothed out the dynamic pressure and angularity distributions. During the fall of 1956 and early winter of 1957 dynamic pressure and angularity surveys were run; the results of which are presented herein. In January 1957 work began on setting up the hot-wire equipment which was to be used for turbulence measurements. A great deal of time and effort was required to

get the equipment in working order, especially the reduction of the amplifier noise level. The hot-wire anemometer was finally considered in working order in late May of 1957. The results of hot-wire measurements made in June, 1957 are also reported herein.

In summary, the purpose of this report is to present representative plots of the final dynamic pressure and angularity surveys as well as free tunnel turbulence data, turbulence data behind grids, and boundary-layer profiles and turbulence on a flat plate (with a roughened leading edge) in the presence of a zero longitudinal static pressure gradient.

EXPERIMENTAL TESTS AND PROCEDURE

A schematic of the low turbulence wind tunnel is shown in Fig. 1. The coordinate system employed to locate stations in the working section has an origin of coordinates located at the entrance to the working section on the tunnel geometric centerline. Positive spatial movements from the origin (with an observer looking upstream) are: upstream (+ X), lateral to the right (+ Y), and vertically upwards (+ Z).

Longitudinal Static Pressure Gradient.

As reported in reference 1 the north side wall of the working section is adjustable by means of five jack screws. Since the calibration was desired for a zero longitudinal static pressure gradient condition a pitot-static tube was installed on the probe carrier and the static pressure measured in one foot increments along the tunnel geometric centerline. Adjustments to the wall contour were made until the longitudinal static pressure gradient approximated the desired zero value. The adjustment of the wall was made holding the fan rpm constant (i.e. constant working section velocity) at several different values of fan speed.

Speed Calibration.

The speed calibration consists of the calibration of the piezometer rings (described in reference 1) against dynamic pressure readings taken by means of a pitot-static tube located on the geometric centerline of the working section. Speed calibrations were made at three longitudinal stations, namely, X = -1, -9, and -18 feet.

Dynamic Pressure Surveys.

Dynamic pressure surveys were made with a pitot-static tube. The surveys were made in lateral planes at three longitudinal stations (X = -1, -9, and -18 feet), and at nine vertical stations, Z = 0 (centerline), $\pm$ 3, $\pm$ 6, $\pm$ 9, and $\pm$ 12 inches. Measurements in the lateral direction were made at Y = 0 (centerline), $\pm$ 3, $\pm$ 6, $\pm$ 9, $\pm$ 12, and + 15 inches. The dynamic pressure surveys were made at a speed of 21 ft/sec.

Angularity Surveys.

Angularity surveys were made with a directional pitot-tube. Angles of attack, α , measured in the vertical plane and angles of yaw, ψ , measured in the horizontal plane were recorded at the stations listed under dynamic pressure surveys at a speed of 21 ft/sec. To an observer looking upstream positive angles of attack correspond to up flow and positive angles of yaw correspond to flow from left to right in a horizontal plane.

Free Tunnel Turbulence.

Turbulence measurements were made using Thiele-Wright, Hot-Wire Anemometer equipment. Three components of turbulence, u', v', and w' were measured in the working section along the geometric centerline at a speed of 21 ft/sec. The u' component was measured using a single wire placed normal to the stream and the v' and w' components were measured using an X probe (two wires) with a 30 degree vertex angle between each wire and the main stream velocity. The wires for both probes were 0.0001 inch diameter platinum wires made by the Wollaston process. The three components, u', v', and w', were measured at nine longitudinal stations

along the tunnel centerline, namely, X = 0, -24, -48, -73, -96, -120, -145, -168, and -192 inches downstream of the entrance to the working section. Since the turbulence measurements were started in June 1957 sufficient time was not available to make more complete studies.

Turbulence Behind Grids.

The measurement of turbulence behind grids has been performed many times and the results correlated with isotropic turbulence theory. In order to get better acquainted with turbulence measurements it was decided that grids should be constructed and the turbulence behind these grids be measured. Thus a check on our equipment could be made by comparing results. In the design of the tunnel a slot at the entrance to the working section was incorporated for the insertion of a grid. Two grids were fabricated using cold-rolled steel round bar stock. The first had a 2 inch square mesh using 3/8 inch diameter rods and the second had a 1 inch square mesh using 3/16 inch diameter rods. Three turbulence components, u', v', and w', were measured behind the grids along the longitudinal centerline of the tunnel at an airspeed of 21 ft/sec. For the 2 inch grid, measurements were made at values of $\frac{X}{M}$ (where M is the mesh length) $\cong$ -10, -20, -40, -60, -80, and -100 and at $\frac{X}{M} \cong$ -5, -15, -30, -45, -60, -75, -90, -105, -120, -135, for the 1 inch grid.

Turbulent Boundary-Layer On A Flat Plate With Zero Longitudinal Static Pressure Gradient.

In order to simulate a flat plate with a zero longitudinal pressure gradient, a 24 ST aluminum plate was mounted vertically in the working section. The plate spanned the tunnel in the vertical plane and was

held in place by flush bolts which tied the plate to 2" x 2" angles attached to the floor and ceiling. The angles were located on the back side of the plate, i.e. the face of the plate not used as a working face. The leading edge of the plate was feathered on the back side of the plate so as to give a fairly sharp leading edge. Adjustment of the plate contour in the longitudinal direction was made possible by the addition of spacers between the plate and the angles. The plate was levelled in the longitudinal direction and adjustment of the moveable wall (which faces the working face of the plate) gave the desired zero longitudinal static pressure gradient. In order to insure a turbulent boundary-layer on the working side of the plate, coarse grain (36X) sandpaper of 3 inch width and extending from the floor to the ceiling was glued to the plate at a position immediately downstream of the plate leading edge.

Mean velocity boundary-layer profiles were measured with a total head probe and the hot-wire anemometer. The total head probe was constructed from a piece of 1/16 inch I.D. steel tubing with a 0.015 inch wall. The open end of the tube was flattened and the resulting dimensions of the open or flow area were 0.125" x 0.010". The walls were filed so that the centerline of the open area (along the 0.125 dimension) could be positioned 0.010 inch from the wall of the plate. The total head probe was attached to the probe carrier mechanism and positioned to 0.010 inch ± 0.002 from the plate. A dial gage indicator, sensitive to 0.0001 inch, was also mounted on the probe carrier and by means of a long extension arm, approximately 6 inches, contact with the plate was made. With the probe in position and the reading of the dial

indicator noted the probe could then be moved in any increments desired down to less than 0.001 inch. The total head traverses through the boundary-layer were made at six longitudinal stations, namely, X = -1, -2, -5, -10, -15, and -18 2/3 feet, at a tunnel speed of 21 ft/sec. The mean velocity traverses through the boundary-layer with the hot-wire were performed at the same longitudinal stations at 21 ft/sec. The positioning of the hot-wire was more accurate and is described briefly. An aluminum block 1 inch wide by 2 inches long by 1/2 inch thick was coated with Prussian Blue on one 1/2 x 2 face. The block was set on a surface plate and a line scribed along the 2 inch dimension. The position of this line was measured using "jill" blocks. Once the position of the line was known, the face of the block which comes in contact with the plate was coated with a very thin film of grease, and the block then laid against the flat plate with the blued-face facing downstream, and the line on the blued-face running vertical and parallel to the plate. A transit was set up at the exit of the tunnel and with the use of a spotlight, the line on the blued face of the block could be distinctly observed. The hot-wire, being vertical and parallel to the plate, was then advanced toward the plate. The wire was advanced until it lined up with the line on the face of the block. The dial indicator was also installed so that it could be read with the transit at the same time the hot-wire was lined up with the reference line on the block. The thickness of the reference line on the block was essentially that of the Wollaston wire with the silver coating, approximately 0.0025". Thus knowing the position of the reference line to within $\pm$ 0.001" it is

estimated that the probe could be positioned to within $\pm$ 0.002". The probe was then moved in and out by the carrier mechanism and its position read from the dial gage indicator. In order to move the probe in 0.001" intervals an extension rod, running under the tunnel from the probe carrier drive motor to the tunnel exit, was designed to engage the motor drive and could be turned at the tunnel exit. The gearing of the motor drive and the probe carrier was such that one revolution of the extension rod corresponded to 0.0005" travel of the probe. Turbulence measurements of the axial component, u', were made during the runs and at the same time that the mean values of the velocity profiles were measured.

RESULTS

Longitudinal Static Pressure Gradient.

The longitudinal static pressure distribution along the tunnel geometric centerline is shown in Fig. 2. Two curves are shown, one for the free tunnel at a speed of 25 ft/sec. and a second for the condition wherein the flat plate is mounted in the tunnel with the speed set at 21 ft/sec. The ordinate, Δh_p, represents the difference in static pressure at the X = 0 station and each downstream axial station. In each case the data indicate that essentially a zero longitudinal static pressure gradient can be set since variations of $\pm$ 0.002 inch of alcohol are the maximum deviations observed. On the basis of the data shown in Fig. 2 it is felt that arbitrary pressure gradients could be set up within $\pm$ 0.002 inch alcohol for the range of movement available from the moveable wall. This range is approximately $\pm$ 21 inches for each jack-screw shown in Fig. 1. Tests at 70 ft/sec. were run holding the wall in its correct position for U_1 = 21 ft/sec. The results indicate static pressure variations of $\pm$ 0.0045 alcohol from the mean. However, small changes in the wall position would bring these pressure variations down to $\pm$ 0.002 inch of alcohol.

Speed Calibration.

The results of the speed calibration are shown in Fig. 3 as a plot of piezometer pressure, h_{p_z}, versus indicated airspeed. The data shown are for longitudinal stations, X= -1, -9, and -18 feet from the

working section entrance. The data indicate that a single curve can be used for setting the speed for any longitudinal station. Small deviations exist because the wall setting was not changed as the tunnel speed was changed. However, it is believed that if the wall were adjusted for each tunnel speed that a single curve of h_{p_z} vs. V_i would suffice regardless of the longitudinal position.

Dynamic Pressure Surveys.

The dynamic pressure surveys indicate that the variation in dynamic pressure is less than 1/4 of one percent of the centerline value within a central core defined by $0 < X(\text{ft}) < -18$, $-12 < Y(\text{inches}) < 12$ and $-12 < Z(\text{inches}) < 12$. The error arising from the manometer sensitivity is estimated at $\pm$ 0.001 inch of alcohol. Typical plots of dynamic pressure versus position at $U_1 = 21$ ft/sec. are shown in Fig. 4. It is noted that the change in dynamic pressure from the mean is of the order of $\pm$ 0.001 inch of alcohol. Thus for low speeds the changes in dynamic pressure result primarily because of the manometry inaccuracy. At higher speeds the changes in dynamic pressure, h_q inches of alcohol, in the central core are of exactly the same order of magnitude as shown in Fig. 4. However, the absolute value of h_q is increased thus the percentage error is decreased. On this basis it is argued that the changes shown in Fig. 4 result primarily from insensitivity in the manometer setting.

Angularity Surveys.

The angularity distributions looking upstream in the X - Z plane, $\Delta\alpha$ (positive $\Delta\alpha$ is up), and in the X - Y plane, $\Delta\psi$ (positive $\Delta\psi$ is

from left to right), are shown in Figs. 5 and 6, respectively. The data for these plots were taken at an airspeed of 21 ft/sec. with the value of α and ψ at the centerline being used as reference or zero values; thus the angularities at each lateral station are plotted as delta values. In Fig. 5 it is noted that the angularity, α , stays within $\pm$ 0.25 degrees at X = -1 and -9 foot stations but exceeds these values slightly at the X = -18 foot station. The larger values of $\Delta \alpha$ at X = -18 feet are attributed to the proximity of the open working section (free jet) at the tunnel exit. The plots of yaw angle, $\Delta \psi$, in Fig. 6 exhibit the same tendencies as the $\Delta \alpha$ distributions except that the yaw angle deviation approaches $\pm$ 1 degree at the X = -18 foot station. Upstream of the X = -18 foot station the angularity surveys indicate acceptable deviations from centerline values.

Free Tunnel Turbulence.

The free tunnel turbulence components u', v', and w' were measured along the geometrical centerline of the working section. Plots of these data taken at U_1 = 21 ft/sec. are shown in Fig. 7. At the working section entrance the data show intensity levels which are essentially the same for all three components. As the hot-wire is moved downstream the intensity of each component increases and reaches a maximum as the working section exit is approached. The vertical component, w', shows the largest increase in intensity at the X = -18.7 foot station and the lateral, component, v', shows the smallest increase at this station. It should be pointed out, that the increase in turbulence as the probe is moved downstream is probably due to the wakes coming off the open channels

which are used to support the probe carrier mechanism. Assuming that the turbulent wakes from the channels diverge at a 7 degree angle would result in the intersection of these wakes at approximately X = -12 feet. Thus it can probably be assumed that the increase in turbulence, as the probe is moved downstream, results from the interaction of the channel wakes with the main stream. In the future these channels will be covered in order to minimize the effect of these turbulent wakes on the free tunnel turbulence. Unfortunately, sufficient time was not available to evaluate the effect of the channels during the present program. With the channel wakes present the turbulence level is considered acceptable for low turbulence work at longitudinal positions upstream of X = -15 feet since the turbulence level does not exceed essentially 0.057 percent of the main stream velocity.

Turbulence Behind Grids.

The decay of turbulence behind 1 and 2 inch square mesh grids was measured at an airspeed of 21 ft/sec. Three components of turbulence (u', v', w') were measured at various longitudinal stations along the geometric centerline of the working section. Plots of $(U_1/u')^2$, $(U_1/v')^2$, and $(U_1/w')^2$ vs. $\frac{X}{M}$ are shown in Fig. 8. The data indicate that the decay of turbulence is essentially linear over the range $20 \lesssim \frac{X}{M} \lesssim 100$. In addition, it can be seen that the condition of isotropy (i.e. $u'^2 = v'^2 = w'^2$) is closely approximated over the range of values of $\frac{X}{M}$ examined, although the values of U_1^2/u'^2 (for the 1" mesh) and U_1^2/w'^2 (for the 2" mesh) appear to deviate from the curve as $\frac{X}{M}$ exceeds 80. This tendency for U_1^2/u'^2 to deviate from a straight line decay is also

exhibited in reference 2. Figure 9 represents a comparison of data on U_1^2/u'^2 from reference 2 and the present tests for 1 and 2 inch square mesh grids. The agreement between the two sets of data is very good over the range $20 < \frac{X}{M} < 60$ which represents the range of $\frac{X}{M}$ examined in reference 2. It should be noted that the Reynolds number (R_{e_M} based on mesh size) for the data in reference 2 is approximately 11,000 and for the present tests is 10,000.

Turbulent Boundary-Layer On a Flat Plate With Zero Longitudinal Static Pressure Gradient.

Measurements of turbulent boundary-layer mean velocity profiles along the vertical centerline of a flat plate with zero longitudinal static pressure gradient were made with a total head probe and a hot-wire anemometer. Typical plots of U/U_1 vs. Y, where U is the mean velocity at a distance Y normal to the plate and U_1 is the freestream velocity outside the boundary-layer, are shown in Figs. 10 and 11 for a working section velocity of 21 ft/sec. The mean velocity profiles (Figs. 10 and 11) measured by the hot-wire and total head probes show reasonable agreement. Fig. 12 represents a comparison of the 1/7 power law for turbulent boundary-layer mean velocity profiles with data taken by total head and hot-wire probes in the present tests. The 1/7 power law gives a good approximation (ref. 3) for the velocity profiles in the turbulent boundary-layer for R_{e_X} from 5×10^5 up to 10^7. The Reynolds number range for the present tests lies between 1.14×10^5 for X = -1 and 2.23×10^6 at X = -18.7. Although the R_{e_X} at the X = -1 and -2 foot stations are slightly below 5×10^5 the agreement of theory and

experiment indicated in Fig. 12 leads to the conclusion that the 1/7 power law adequately defines the velocity profiles for R_{e_X} 5×10^5.

Fig. 13 shows a comparison of boundary-layer thickness, δ, boundary-layer displacement thickness, δ^*, and boundary-layer momentum thickness, θ, measured in the present tests with that of the 1/7 power law. The 1/7 power law values (ref. 3) are given as

$$\delta = \frac{0.37\,X}{(R_{e_X})^{0.2}} \tag{1}$$

where $R_{e_X} = \frac{\rho}{\mu} U_1 X$, ρ being the mass density of air, μ the viscosity of air, and X the longitudinal position on the plate.

$$\delta^* = \int_0^\infty \left(1 - \frac{U}{U_1}\right) dy \tag{2}$$

$$\theta = \int_0^\infty \frac{U}{U_1}\left(1 - \frac{U}{U_1}\right) dy \tag{3}$$

The agreement between experiment and theory is good as expected since the profiles all showed good agreement with the 1/7 power law represented in Fig. 12.

The variation of intensity of the longitudinal turbulence component, u'/U_1, in the boundary-layer is shown plotted in Fig. 14. From the graph it is seen that the intensity reaches its maximum value close to the wall and then falls off as either the wall or the outer edge of the boundary-layer is approached. The data also show that the artificial

turbulence produced by the sandpaper is quite large at the X = -1 and -2 foot stations, and falls off considerably at the X = -5 foot station. The data show that the intensity of the longitudinal component of turbulence is essentially constant for Y/δ = constant from X = -5 to X = -18.7 feet, where the influence of the sandpaper has essentially disappeared.

CONCLUSIONS

From the calibrations and turbulence measurements reported herein, the following conclusions are drawn:

1. The moveable wall can be adjusted to give an arbitrary longitudinal static pressure gradient accurate to within $\pm$ 0.002 inch of alcohol per foot of length over the range of movement of the wall.
2. The dynamic pressure and angularity surveys indicate that the deviations from centerline values are well within desired limits except at the aft end of the working section where the open jet influences the distribution.
3. The intensity of the turbulence components, u', v', and w', in the free tunnel is within acceptable limits. The intensities can probably be further reduced if the channels which support the probe carrier are faired over to eliminate the turbulent channel wakes.
4. The turbulence data measured with the 1 and 2 inch square mesh grids show good correlation with data taken at other facilities thus indicating the reliability of the hot-wire anemometer now in operation.
5. The boundary-layer velocity profiles on the flat plate show good agreement with the 1/7 power law even at Reynold's numbers, R_{θ_x}, below the usually accepted value of 5×10^5. The agreement is interpreted as the existence of a developed turbulent boundary-layer.

6. The intensity of the longitudinal turbulence component in the boundary-layer is seen to be increased in the region, $X < -2$ feet, downstream of the artificial roughness which in these tests consisted of 36X sandpaper. Downstream of the -2 foot station the effect of the sandpaper diminishes rapidly and the intensity as a function of Y/δ shows similar trends between $X = -5$ and $X = -18.7$ feet. This result is expected since similar velocity profiles exist in this range of X positions.

In summary it is felt that the results of the present tests indicate that the tunnel in its present configuration qualifies as a useful tool for turbulence research. The hot-wire equipment is also capable of making the turbulence measurements down to a level of 0.01 percent.

REFERENCES

1. Ducoffe, Arnold L., A Report On the Design, Construction, Operation and Preliminary Calibrations On the Low Turbulence Wind Tunnel at the Georgia Institute of Technology, Navy Department, Office of Naval Research, Contract No. Nonr - 991(01), May, 1956.

2. Batchelor, G. K., and Townsend, A. A., Decay of Isotropic Turbulence in the Initial Period, Proc. Roy. Soc. London, Series A, 1035, July, 1948.

3. Pai, Shih - I, Viscous Flow Theory II - Turbulent Flow, D. Van Nostrand Co., Inc., 1957.

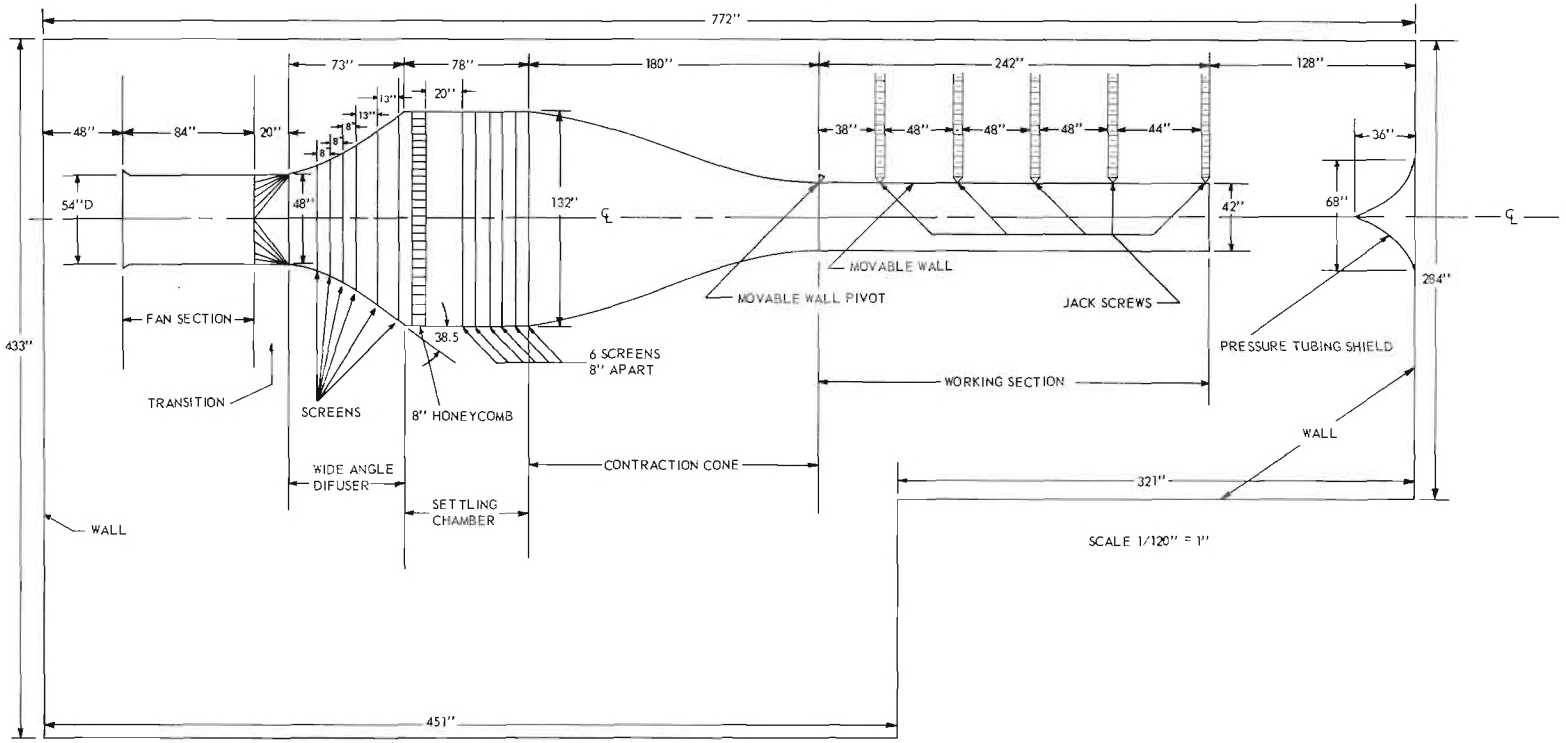

Figure 1. Schematic of Low Turbulence Wind Tunnel.

LONGITUDINAL STATIC PRESSURE DISTRIBUTION

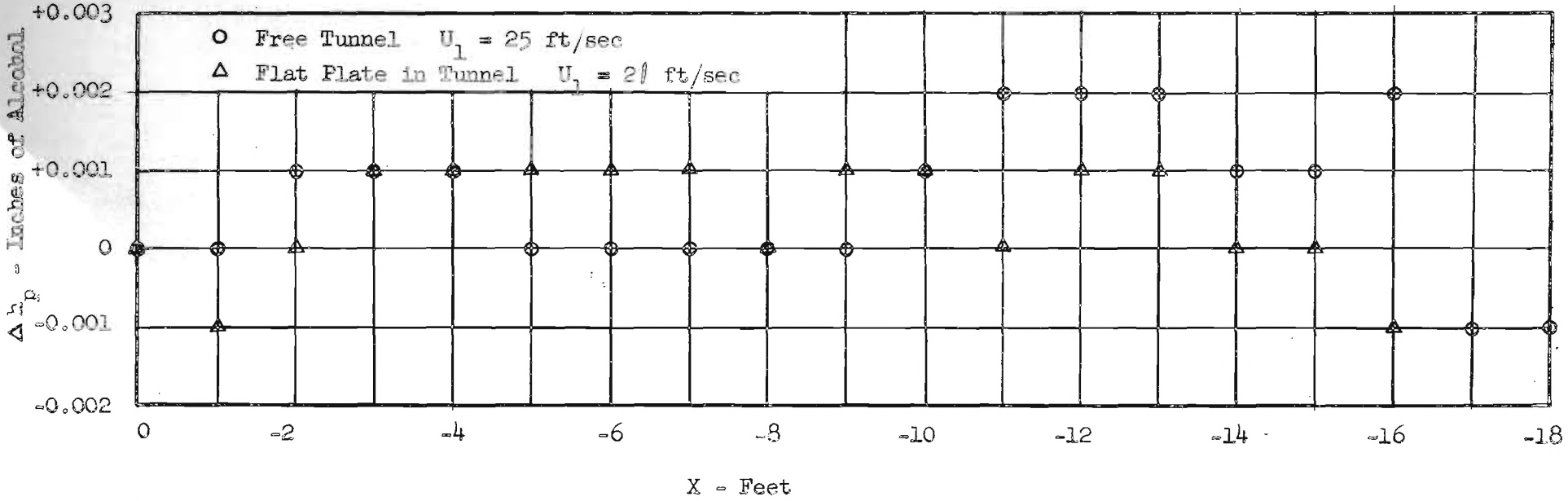

Fig. 2

SPEED CALIBRATION

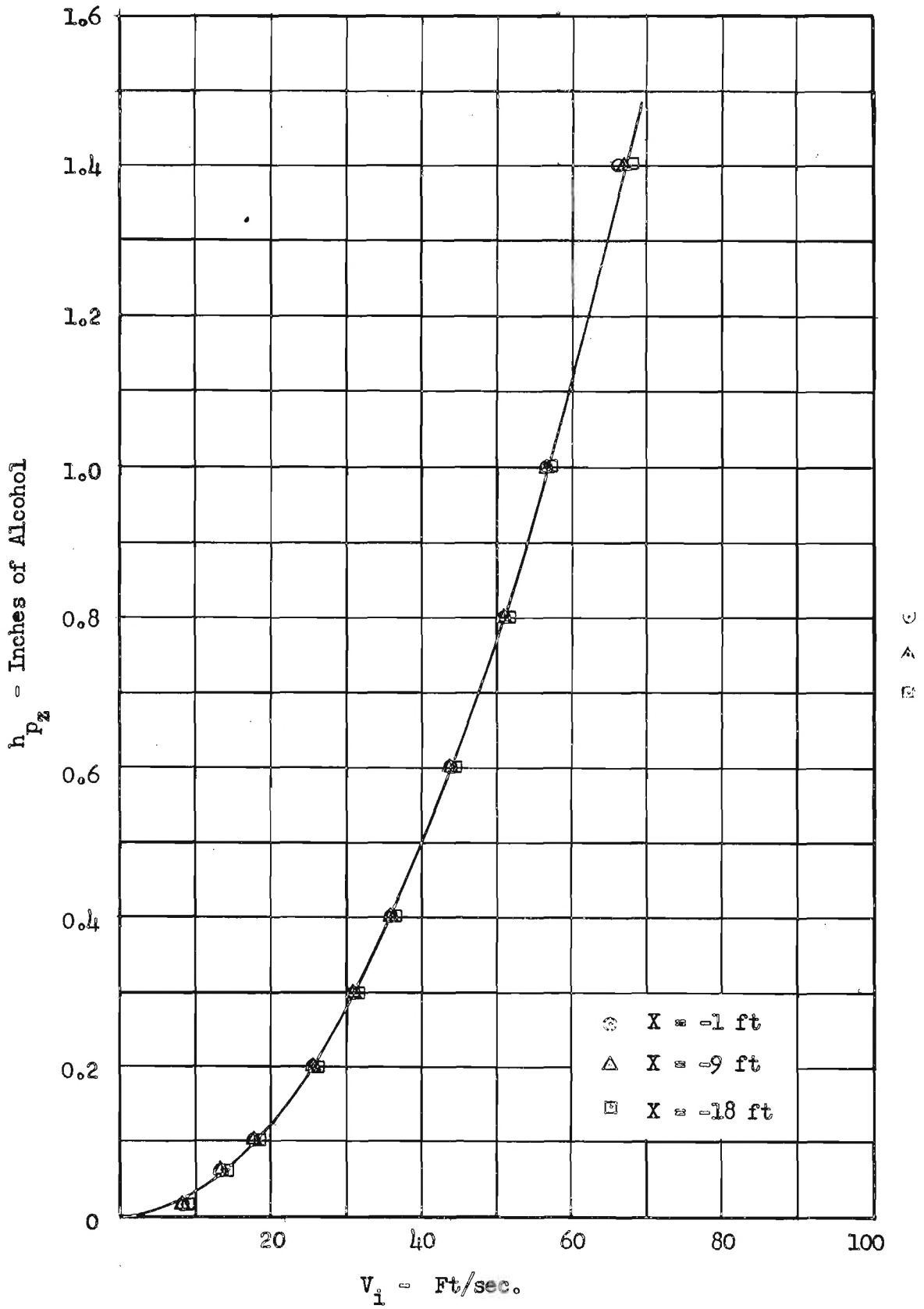

DYNAMIC PRESSURE SURVEYS

U_1 = 21 ft/sec

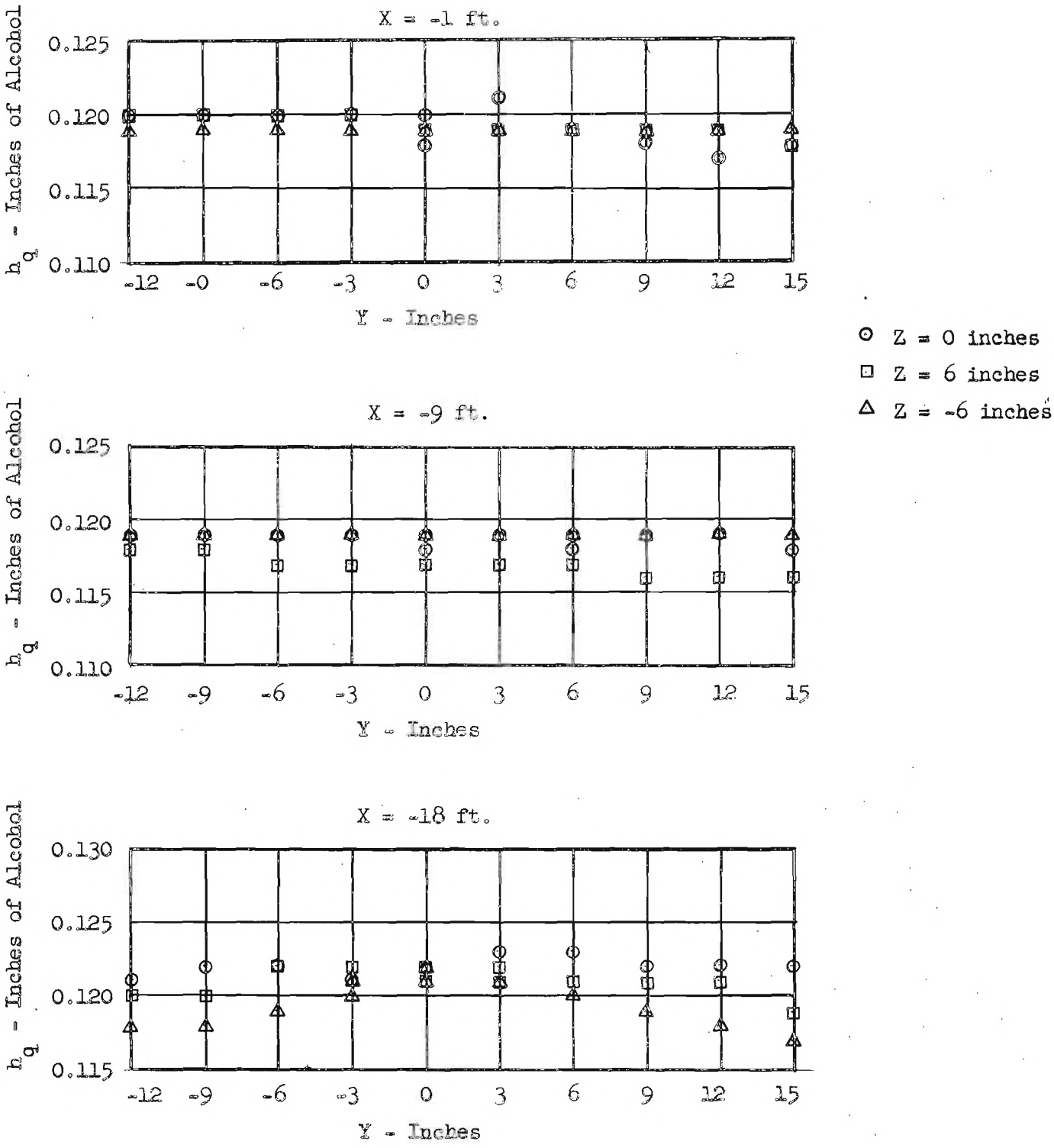

VERTICAL PLANE ANGULARITY DEVIATIONS REFERENCED TO CENTER LINE VALUES

U_1 = 21 ft/sec

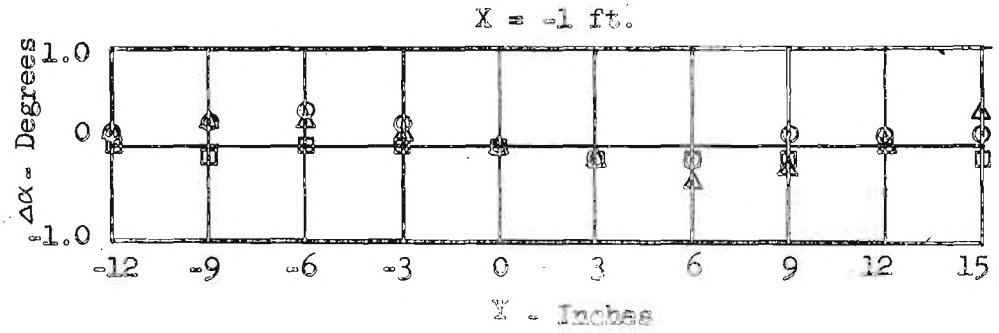

⊙ Z = 0 inches
□ Z = 6 inches
△ Z = -6 inches

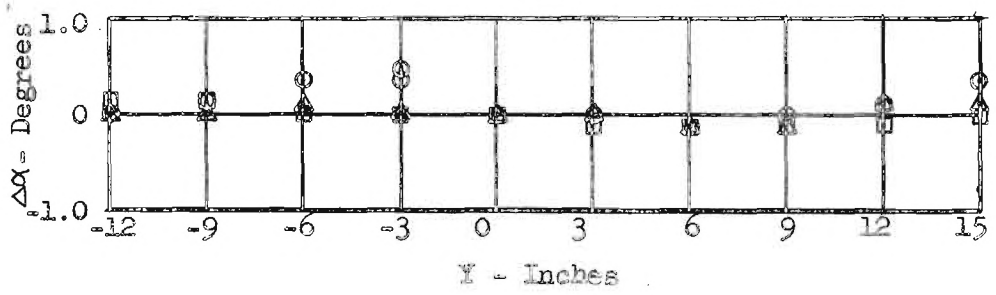

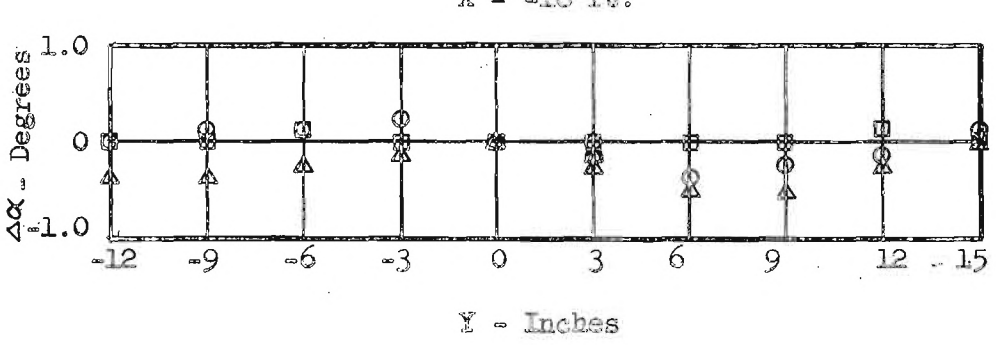

HORIZONTAL PLANE ANGULARITY DEVIATIONS REFERENCED TO CENTER LINE VALUES

U_1 = 21 ft/sec

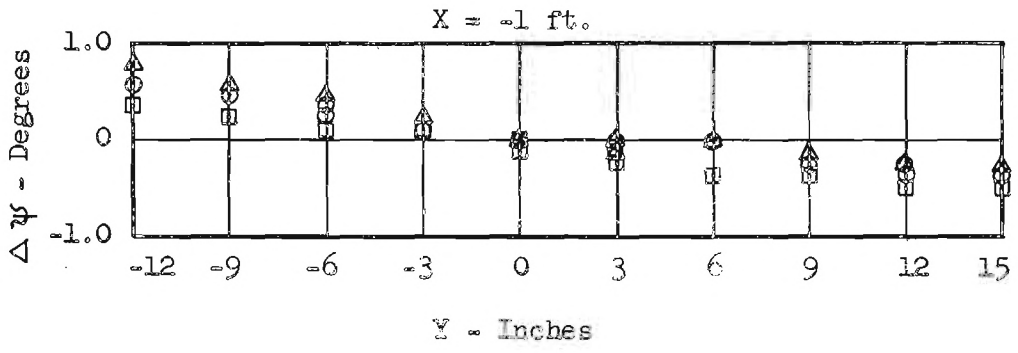

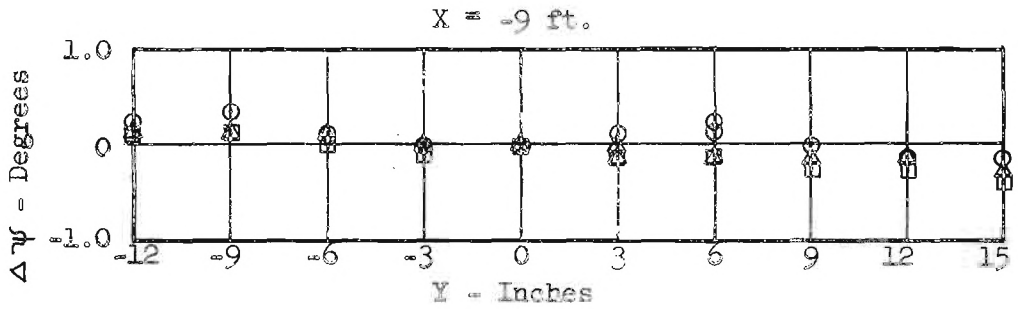

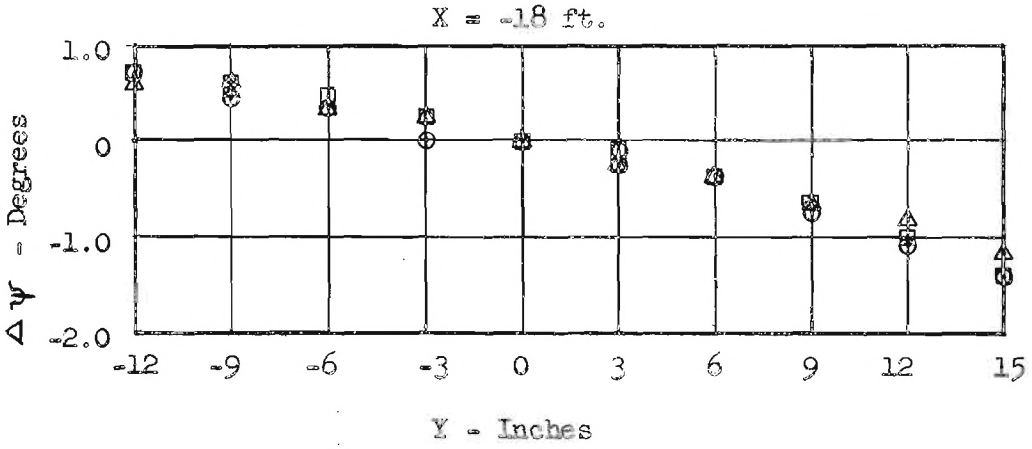

○ Z = 0 inches

□ Z = 6 inches

△ Z = -6 inches

FREE TUNNEL TURBULENCE SURVEYS ALONG
LONGITUDINAL CENTER LINE

U_1 = 21 ft/sec

$\partial h_p / \partial X = 0$

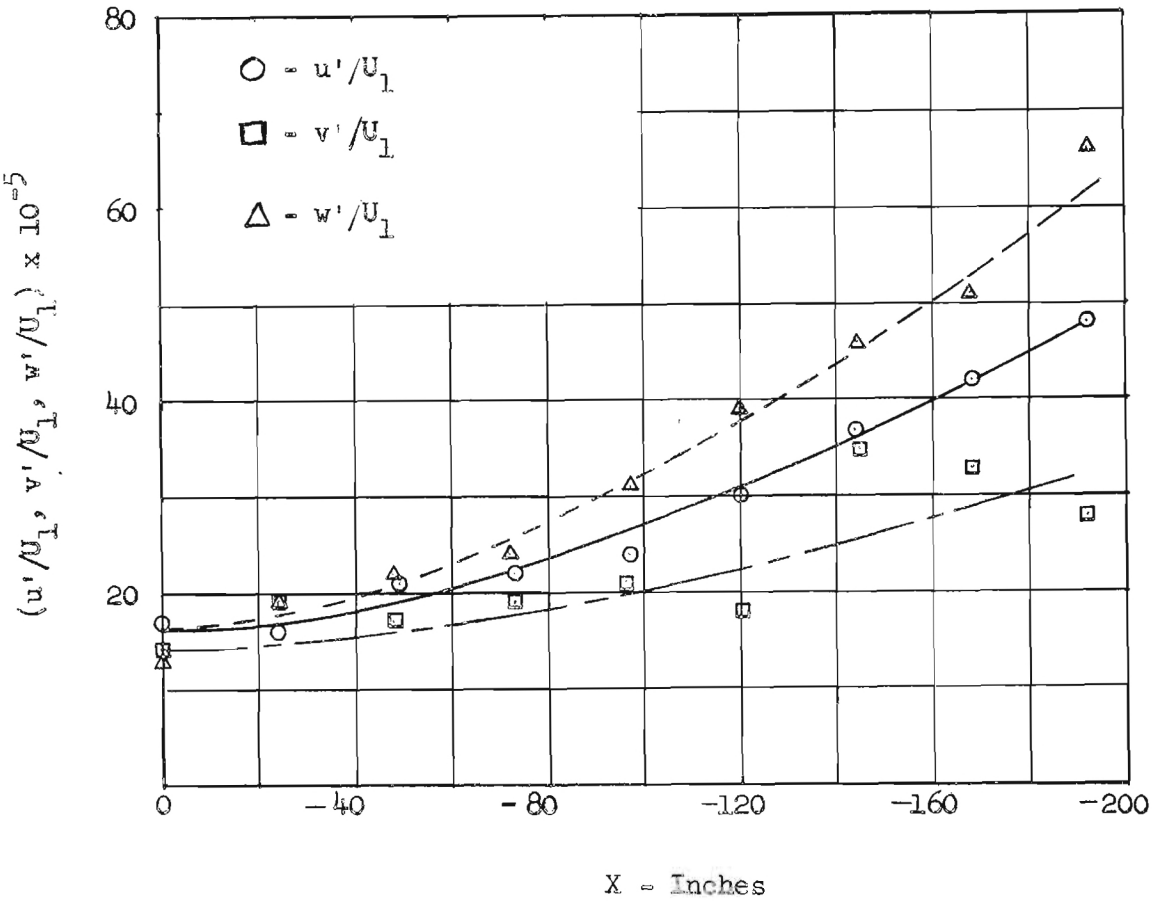

DECAY OF TURBULENCE BEHIND 1" AND 2"
SQUARE MESH GRIDS

$U_1 = 21$ ft/sec

$\partial h_p / \partial X = 0$

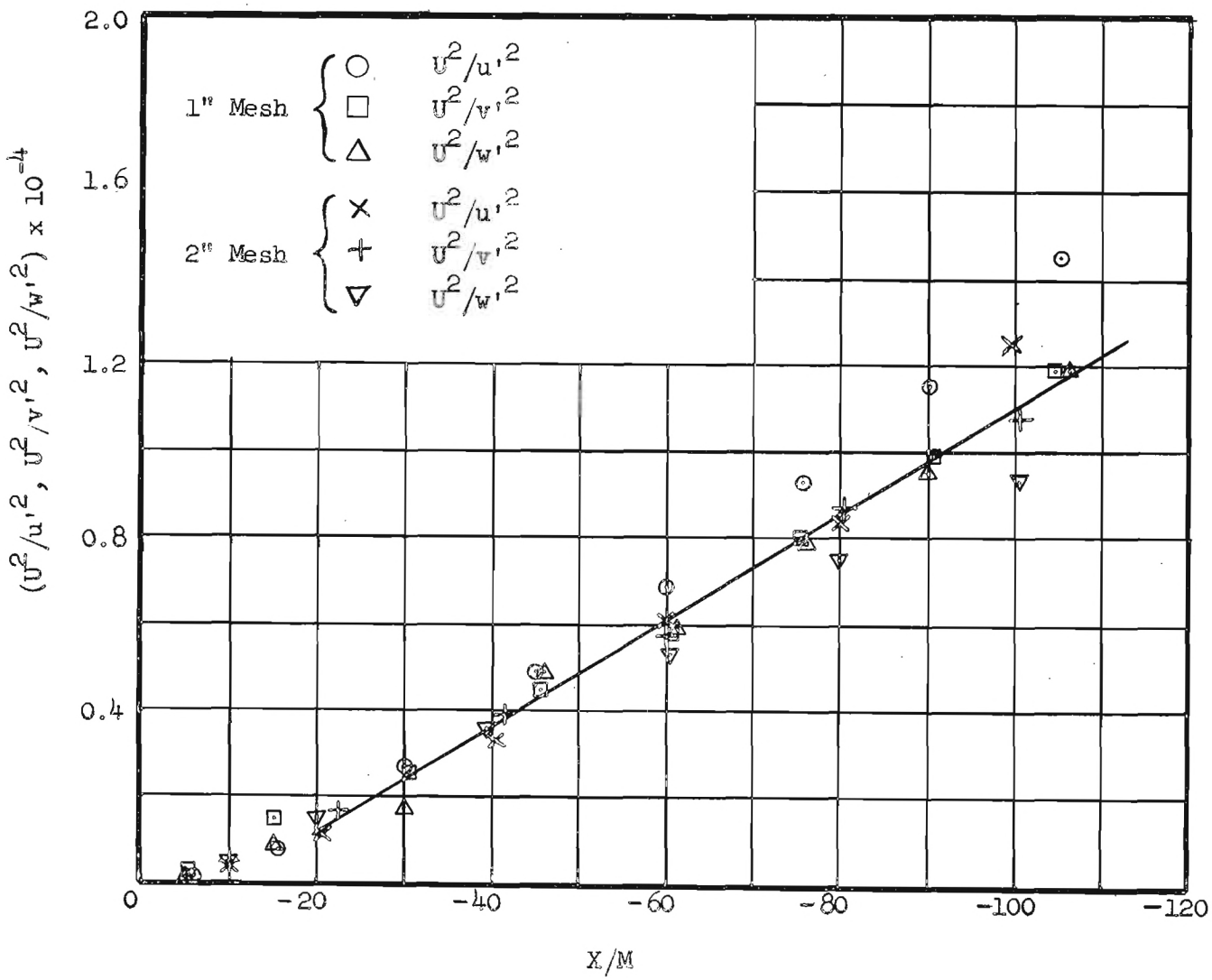

COMPARISON OF LONGITUDINAL TURBULENCE DECAY WITH DATA OF REFERENCE 2 FOR 1" AND 2" SQUARE MESH GRIDS

$U_1 = 21$ ft/sec

$\partial h_p / \partial X = 0$

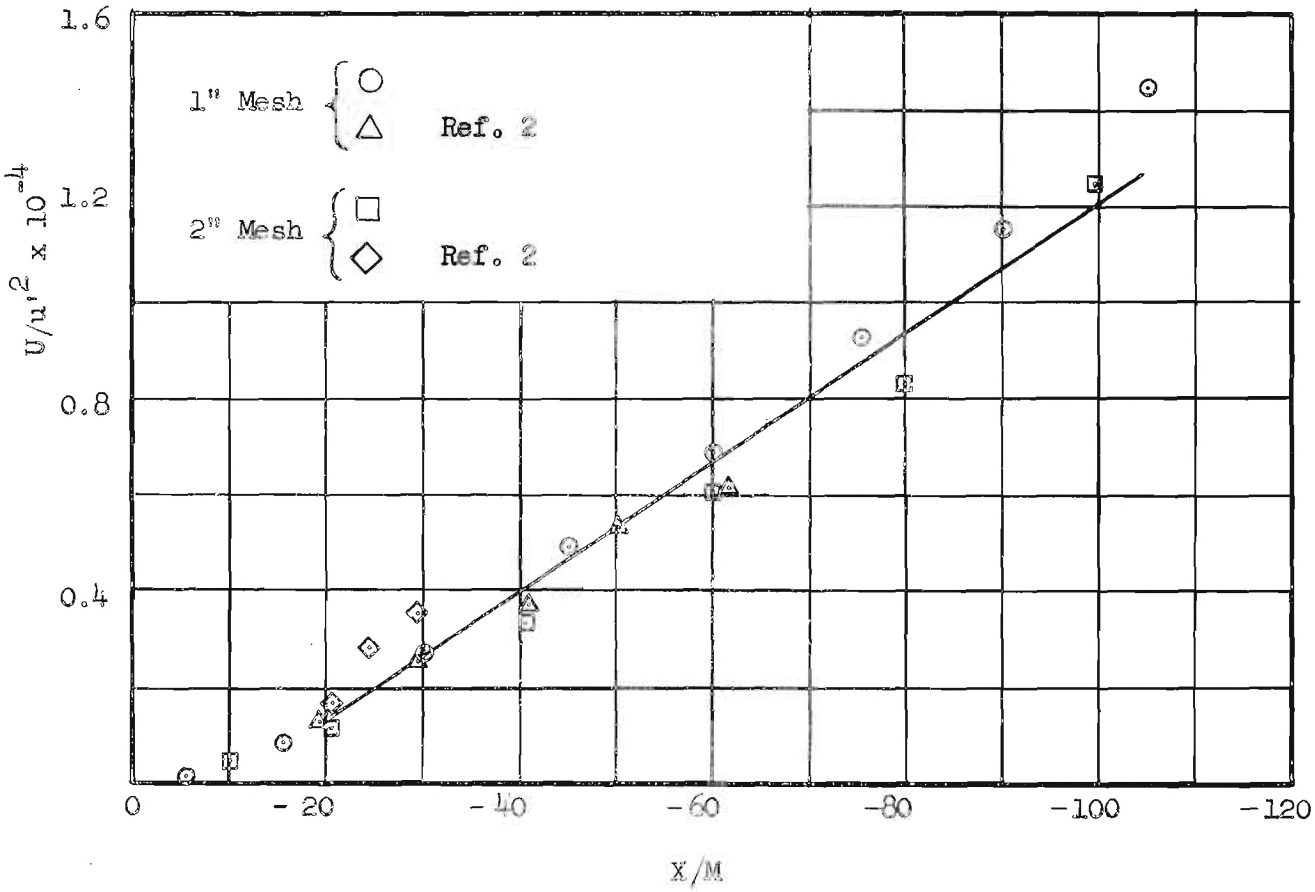

TURBULENT BOUNDARY-LAYER VELOCITY PROFILES

U_1 = 21 ft/sec

$\partial h_p / \partial X = 0$

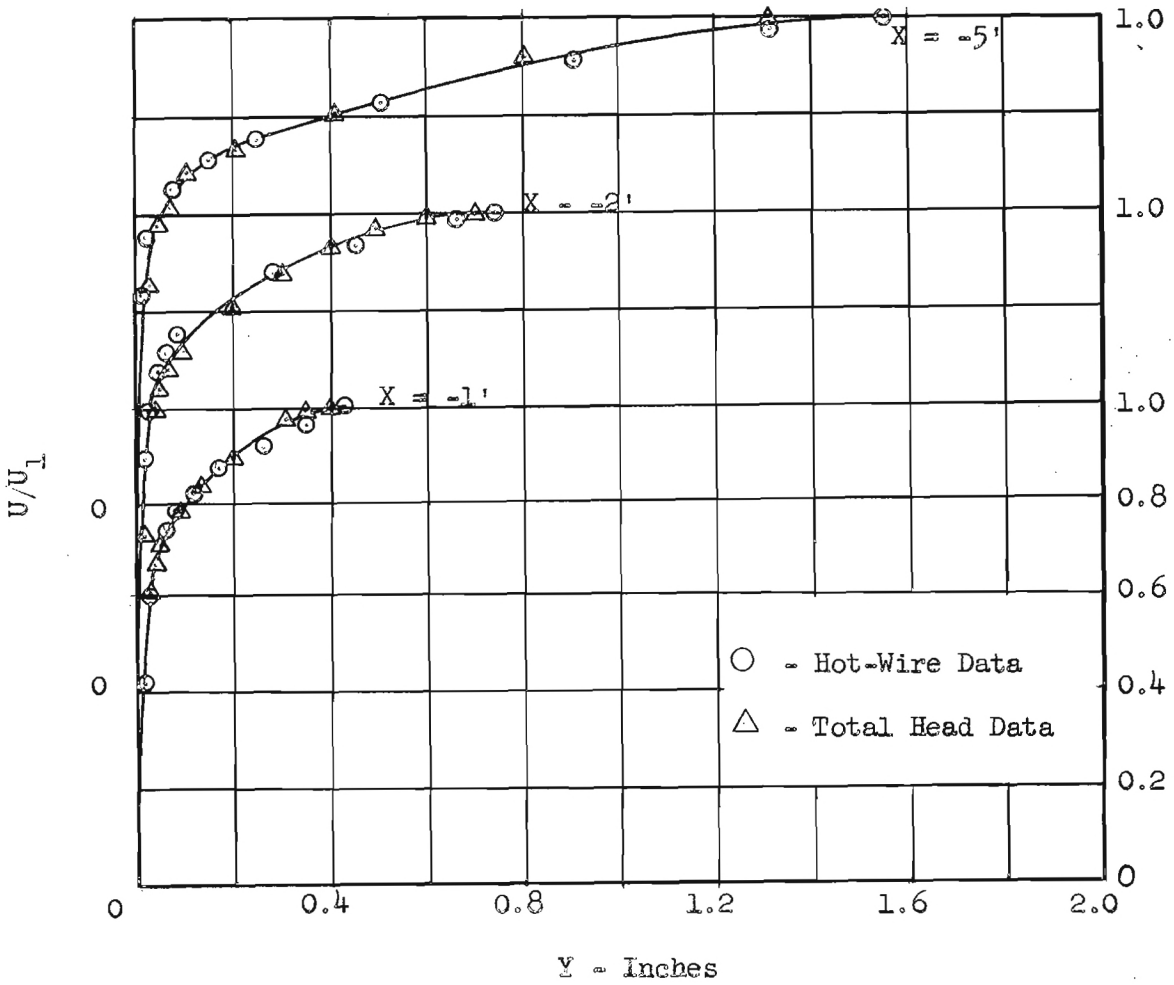

TURBULENT BOUNDARY-LAYER VELOCITY PROFILES

$U_1 = 21$ ft/sec

$\partial h_p / \partial X = 0$

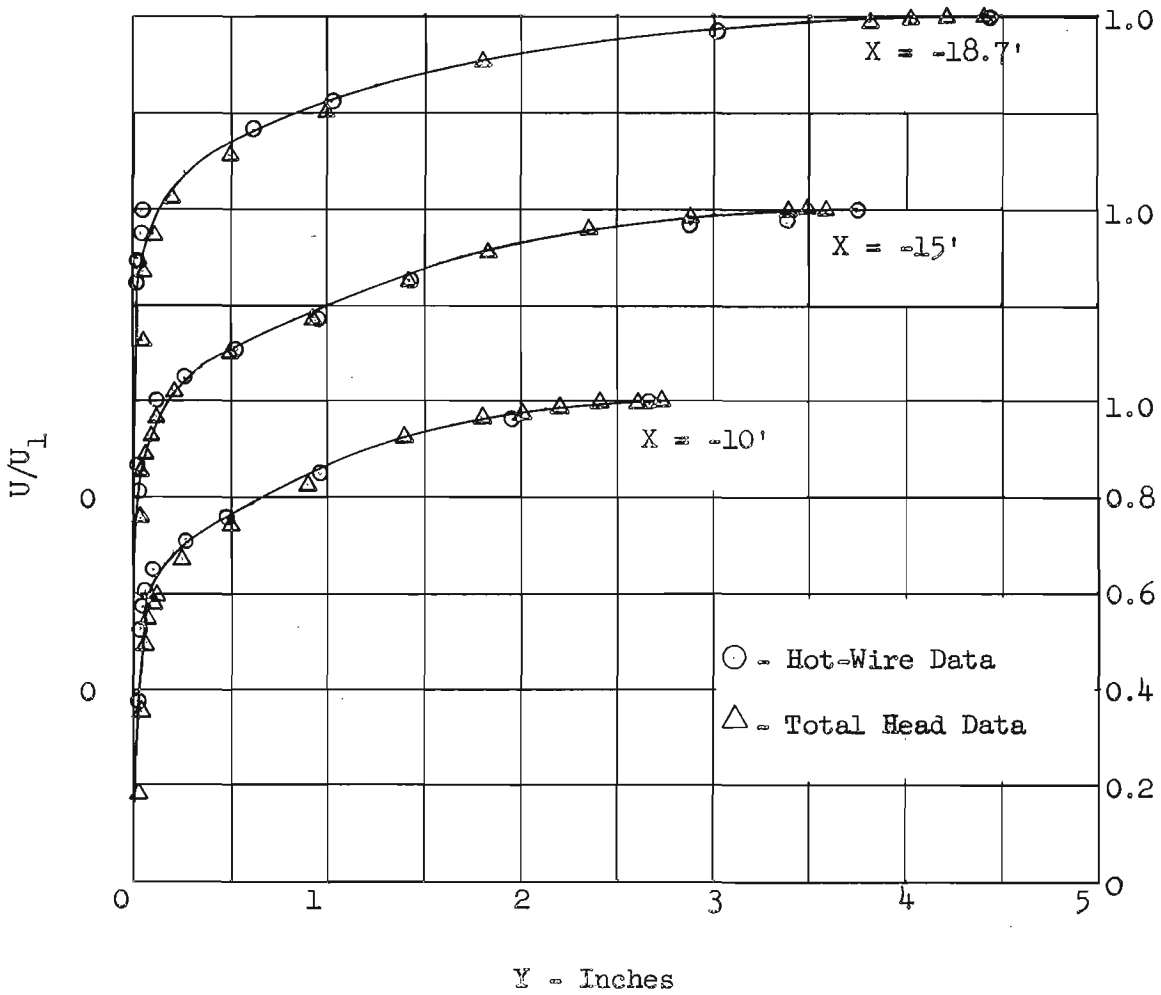

COMPARISON OF MEASURED VELOCITY PROFILES WITH
1/7 POWER LAW

U_1 = 21 ft/sec

$\partial h_p / \partial X = 0$

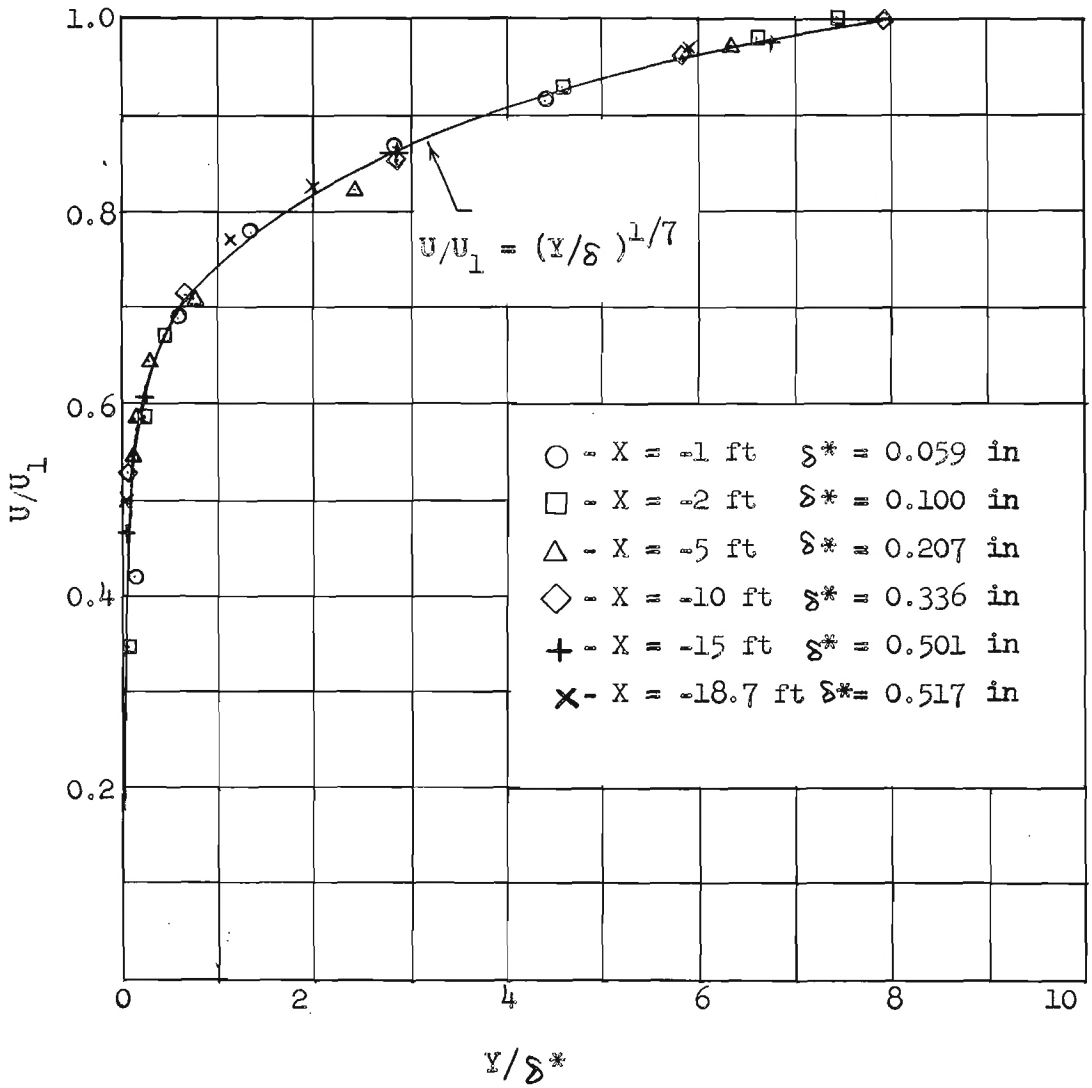

COMPARISON OF BOUNDARY-LAYER PARAMETERS PREDICTED
BY 1/7 POWER LAW WITH MEASURED DATA

$U_1 = 21$ ft/sec

$\partial h_p / \partial X = 0$

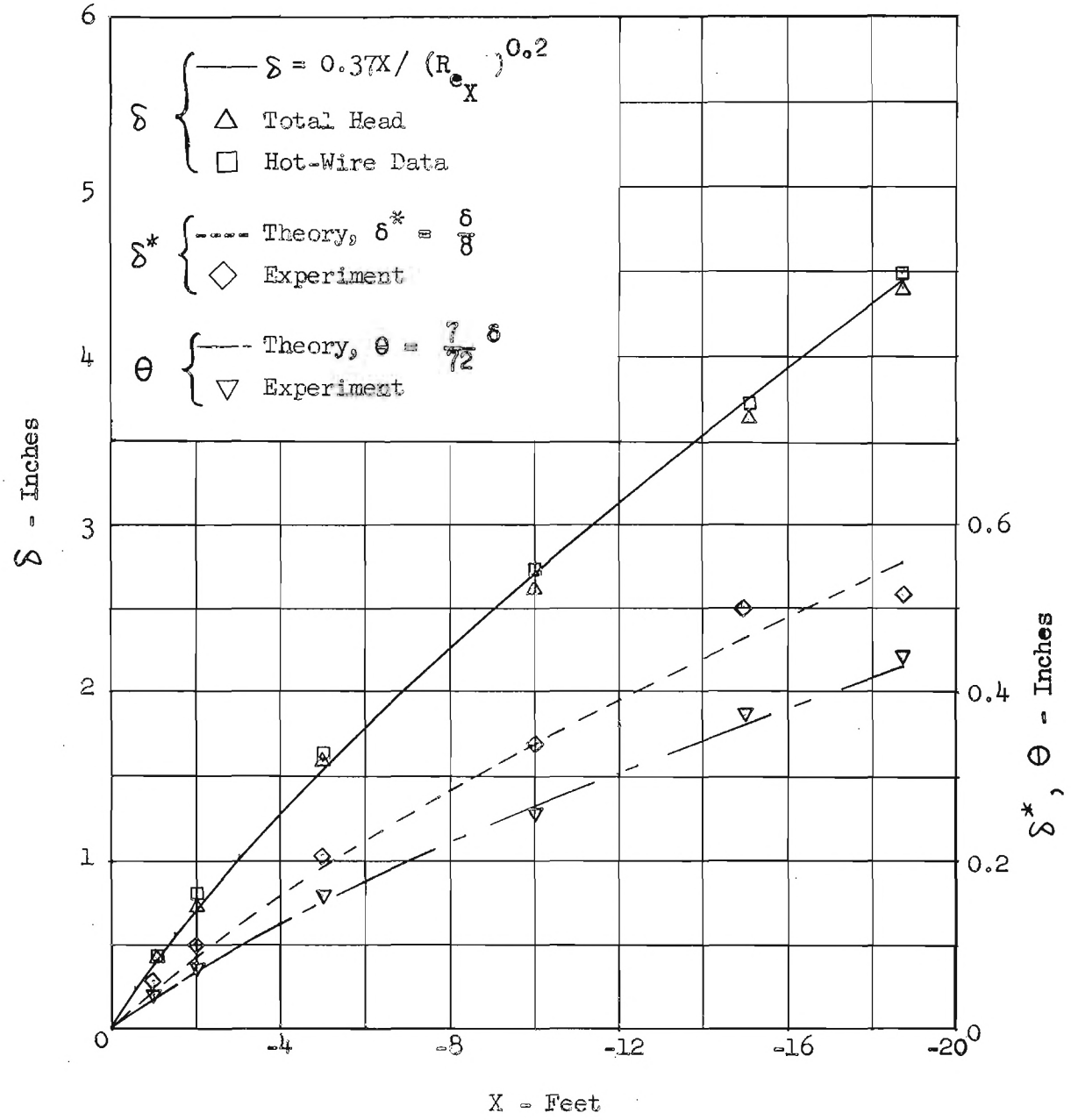

BOUNDARY-LAYER DISTRIBUTION OF INTENSITY OF LONGITUDINAL TURBULENCE COMPONENT

U_1 = 21 ft/sec

$\partial h_p / \partial X = 0$

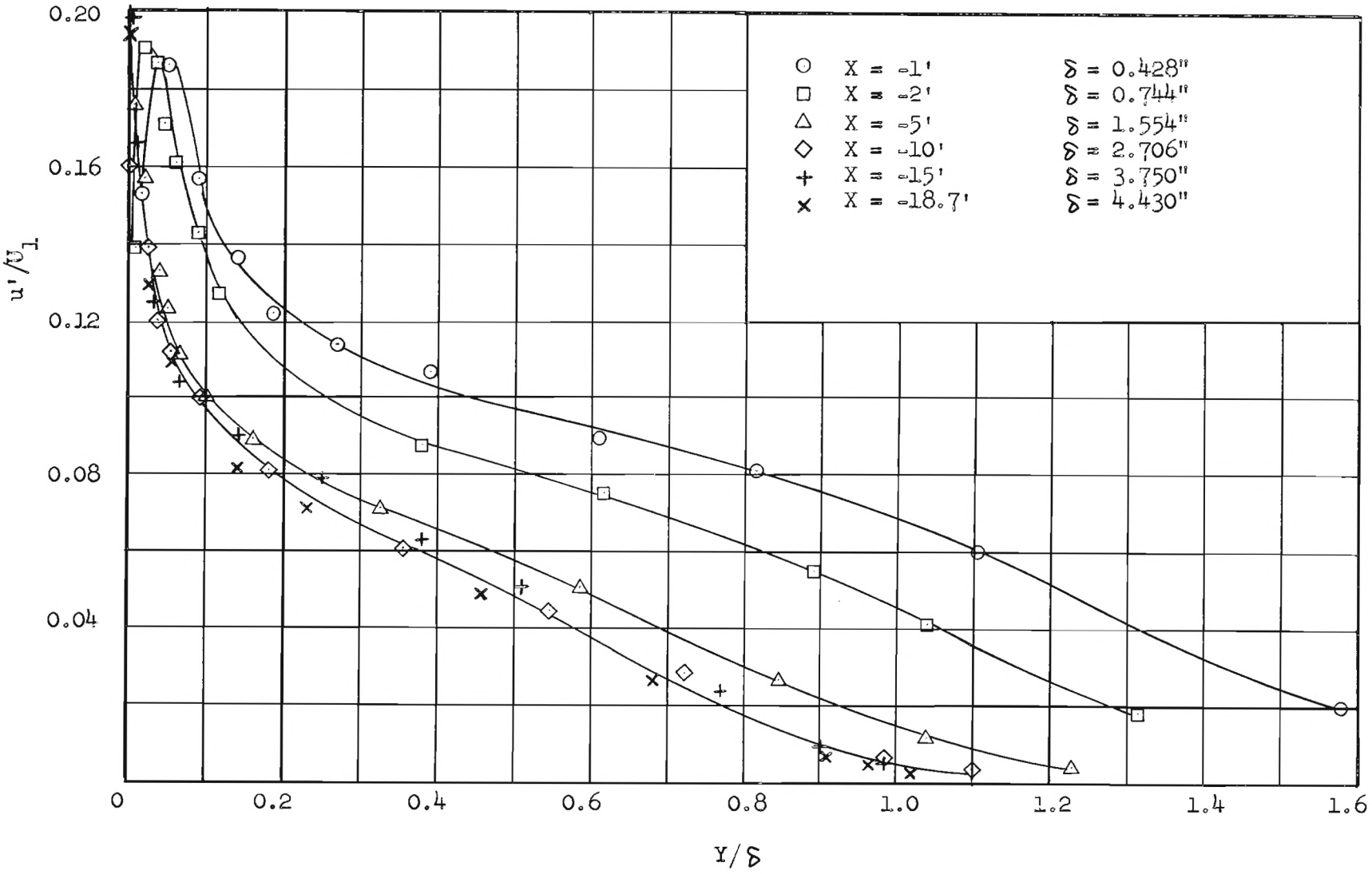

Fig. 14